J Nanopart Res (2013) 15:1613
DOI 10.1007/s11051-013-1613-6

RESEARCH PAPER

Magnetic properties study of iron-oxide nanoparticles/PVA ferrogels with potential biomedical applications

P. Mendoza Zélis · D. Muraca · J. S. Gonzalez · G. A. Pasquevich · V. A. Alvarez · K. R. Pirota · F. H. Sánchez

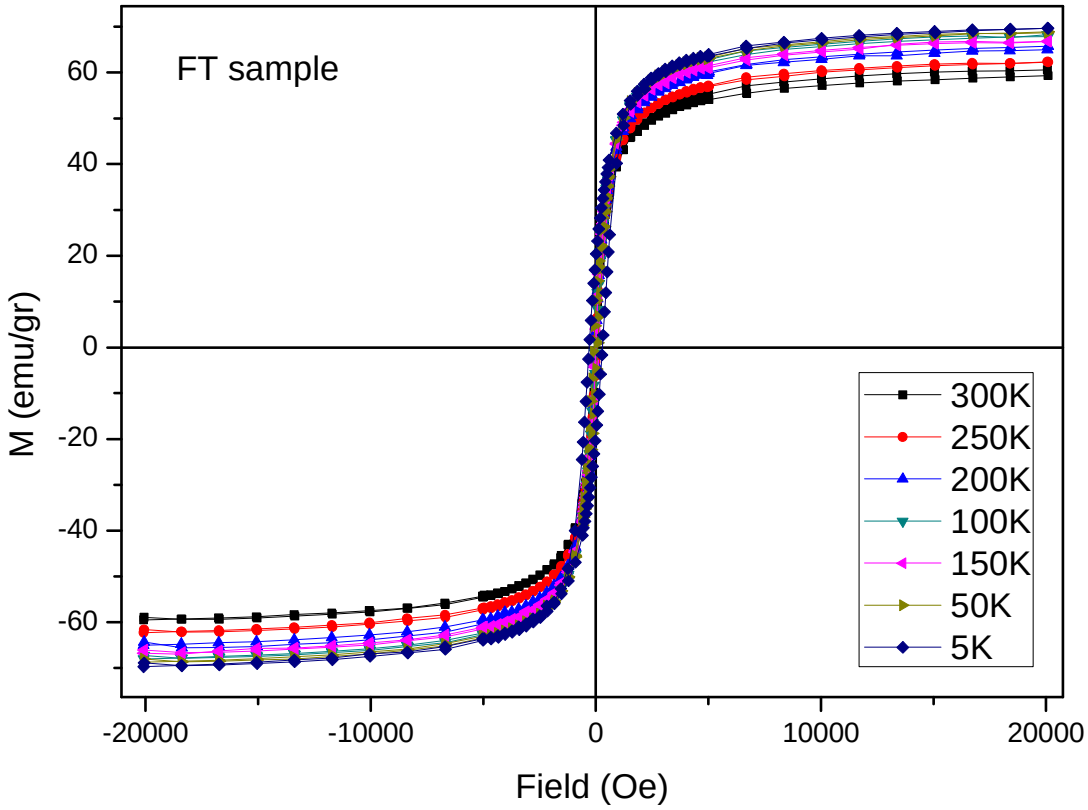
FT sample
M (emu/gr)
Field (Oe)
60
40
20
0
-20
-40
-60
-20000
-10000
0
10000
20000
300K
250K
200K
100K
150K
50K
5K

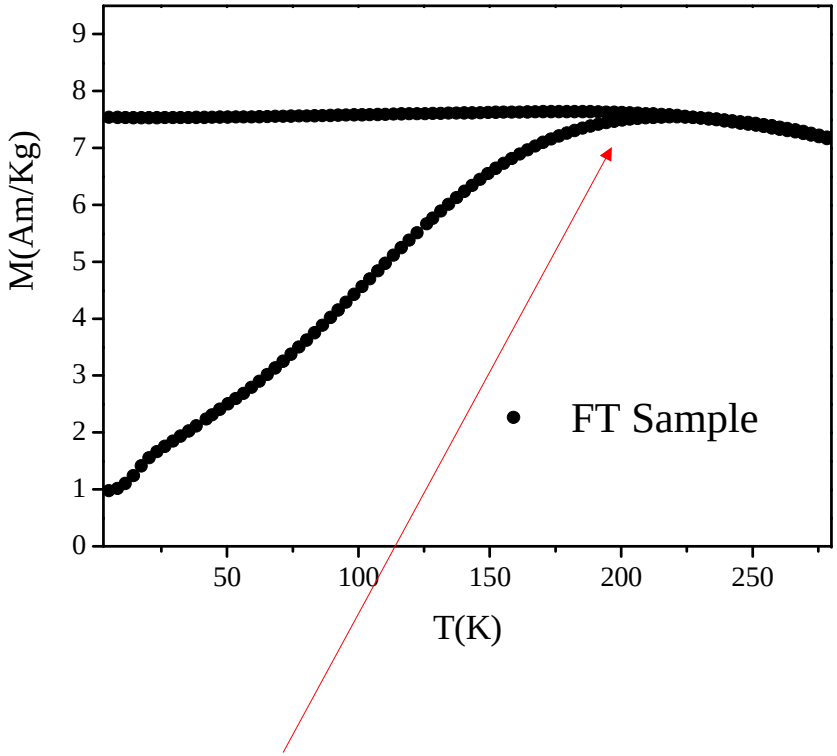

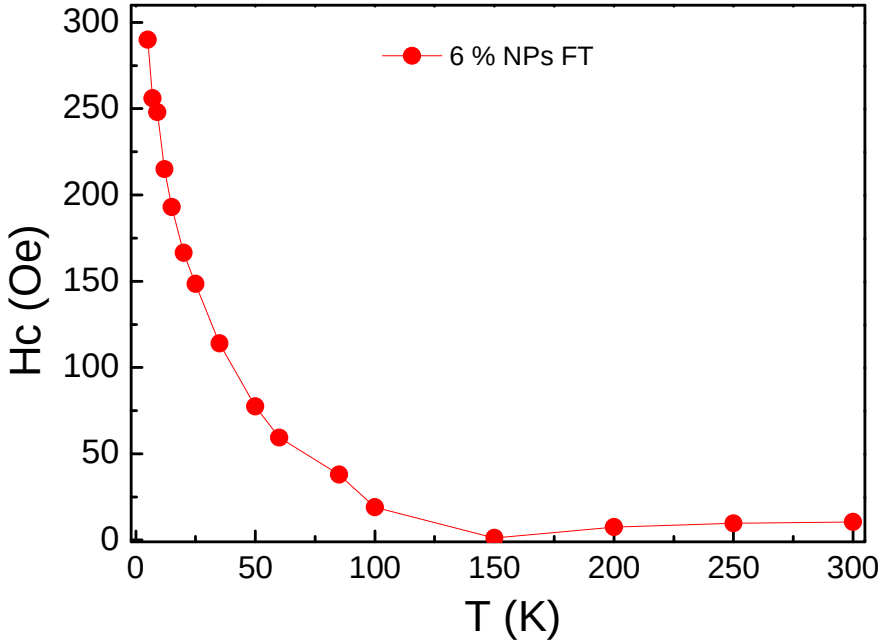

$T_i \approx 200K$

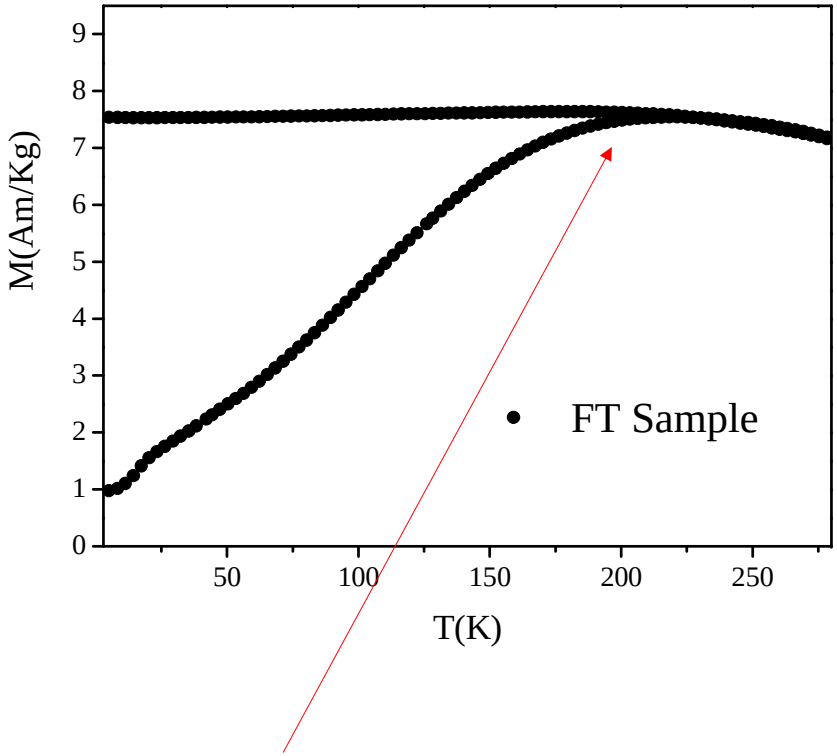

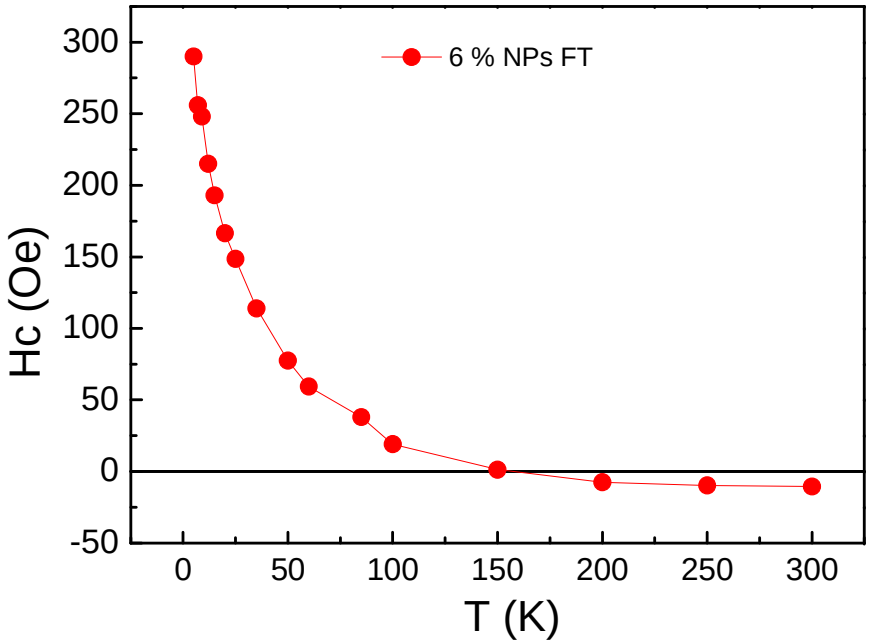

$T_i \approx 200K$

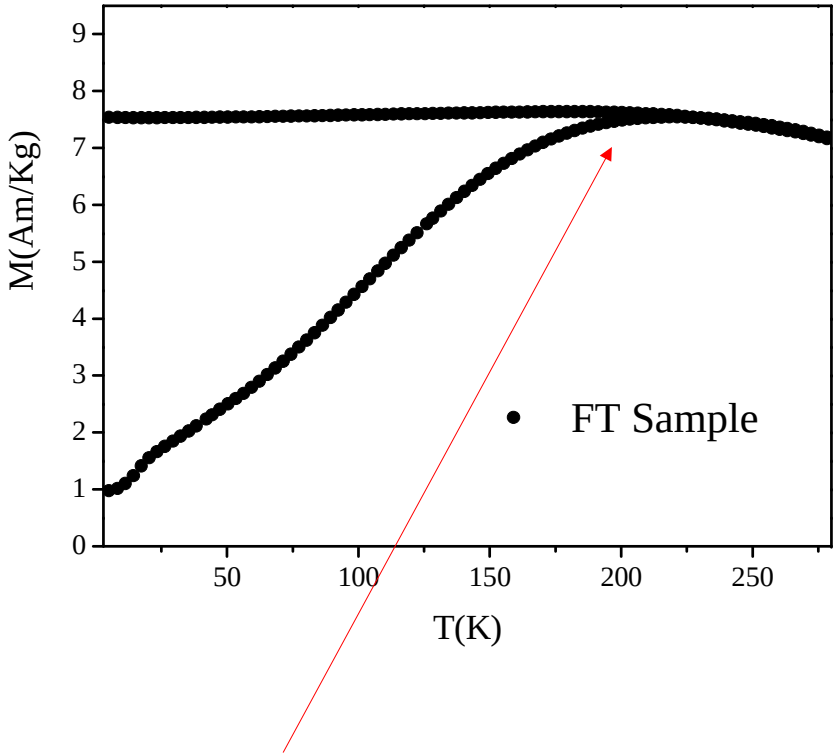

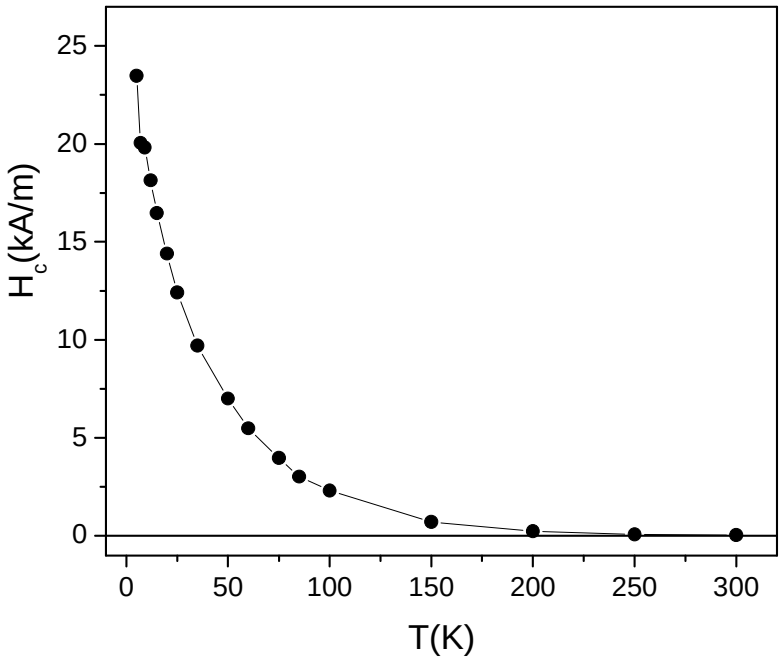

$T_i \approx 200K$

$$M^L = \int_0^\infty \mu^L L\left(\frac{\mu_0 \mu^L (H - H_c)}{k_B T}\right) f(\mu^L) d\mu^L$$

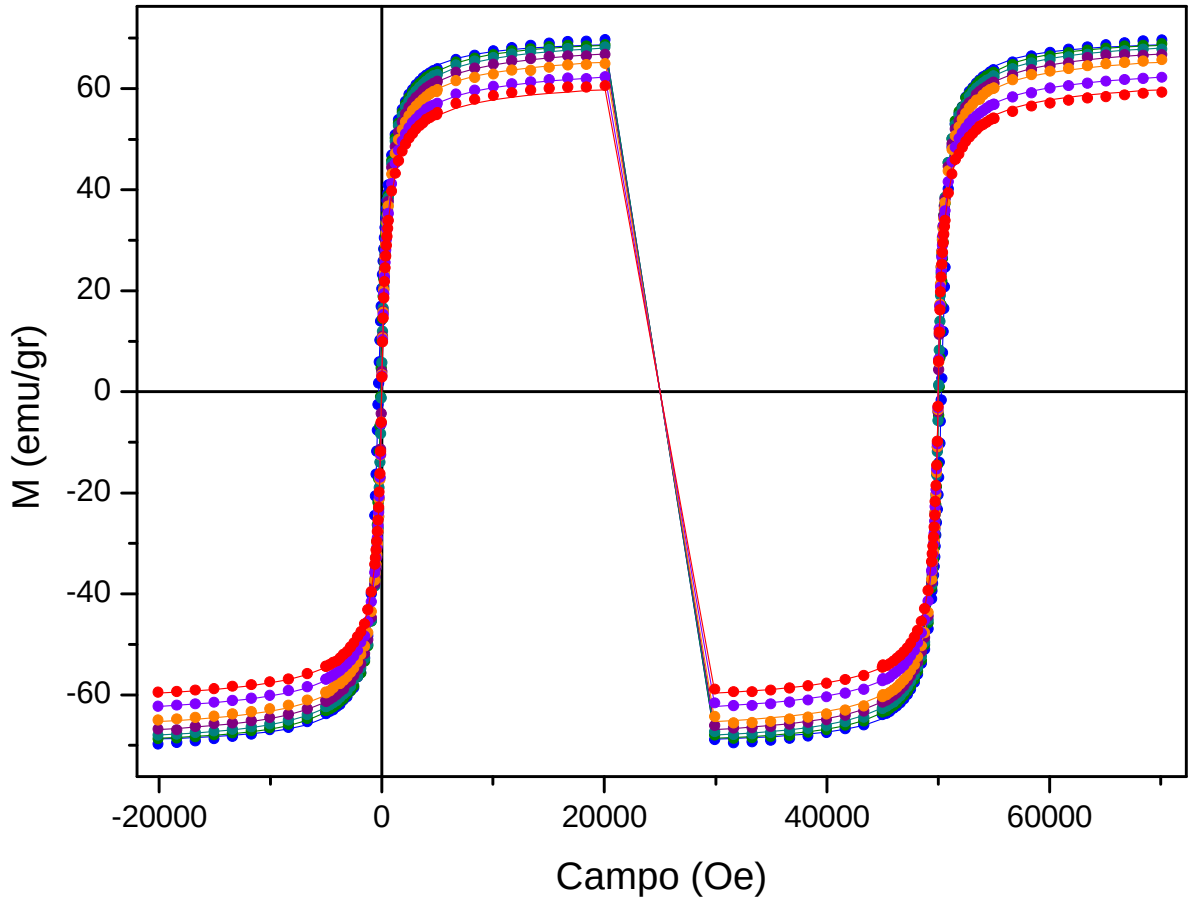

$$M^L = \int_0^\infty \mu^L L\left(\frac{\mu_0 \mu^L (H - H_c)}{k_B T}\right) f(\mu^L) d\mu^L$$

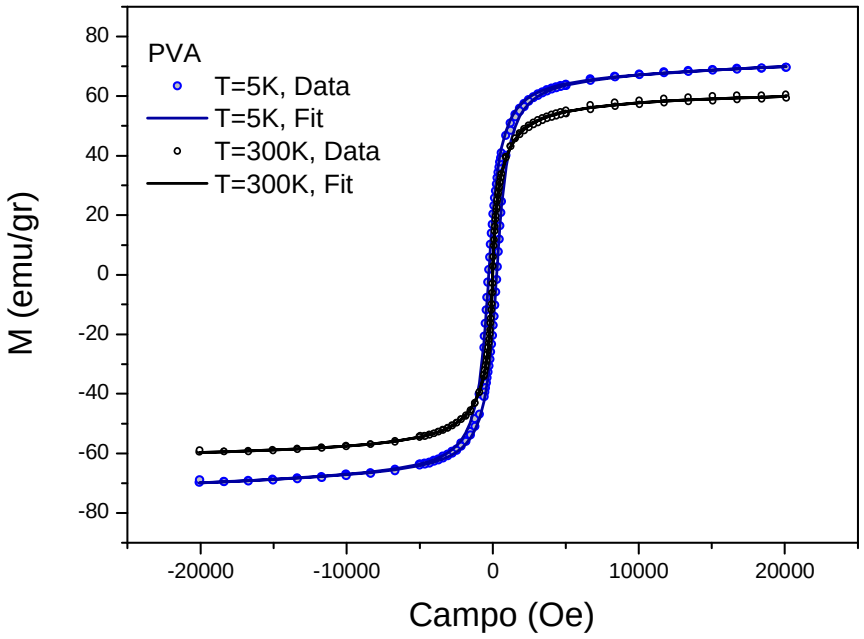

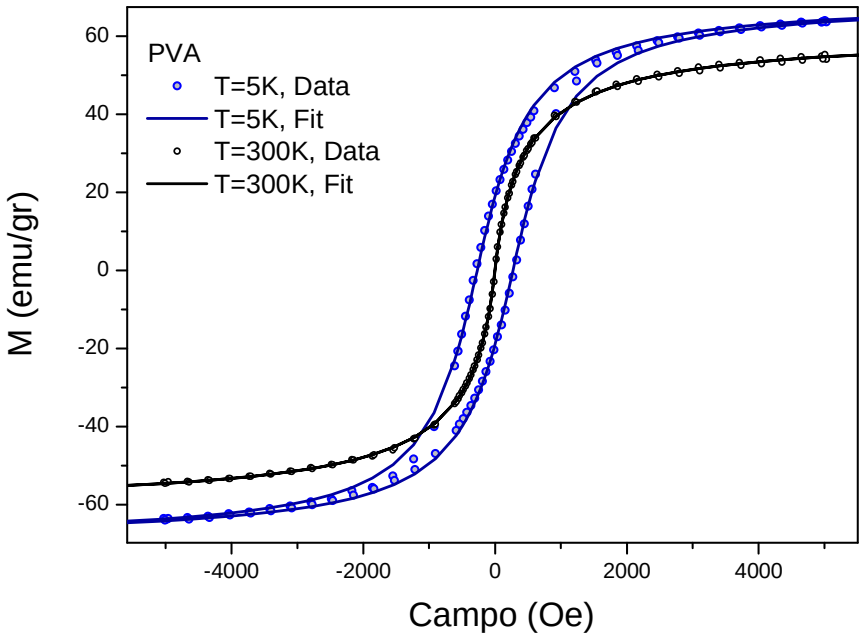

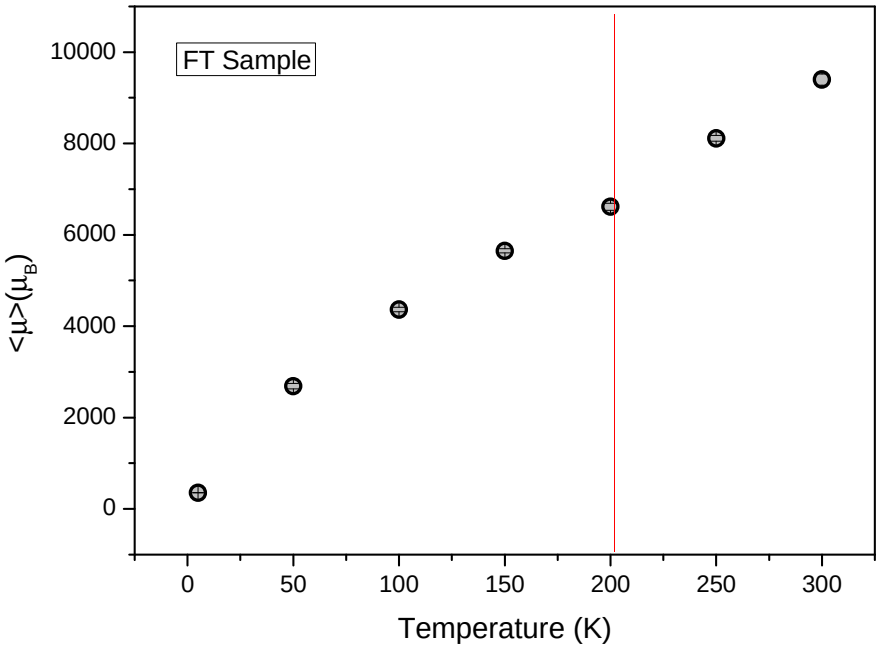

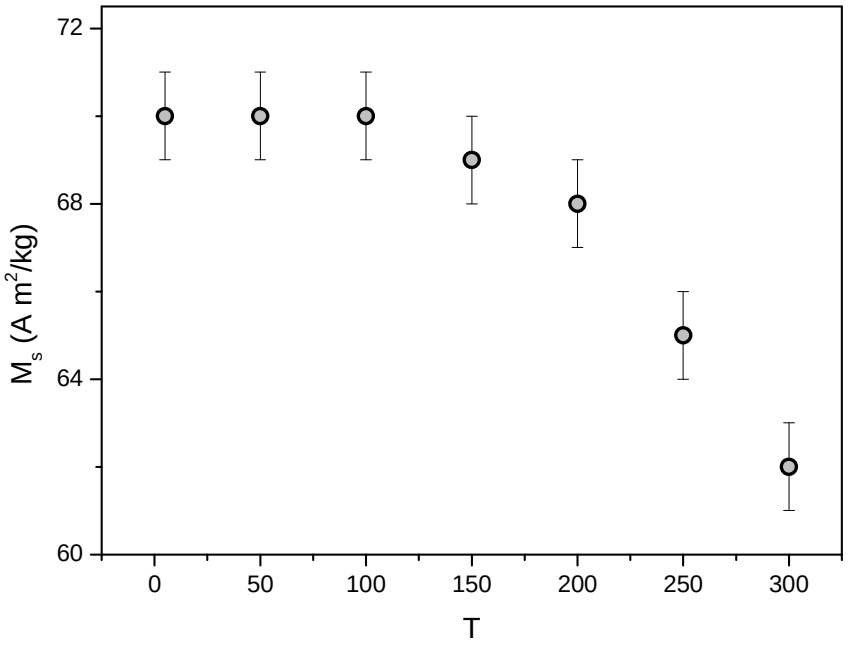

$T_i \approx 200K$

PHYSICAL REVIEW B, VOLUME 64, 144420

Granular Cu-Co alloys as interacting superparamagnets

Paolo Allia,[1] Marco Coisson,[2] Paola Tiberto,[3] Franco Vinai,[3] Marcelo Knobel,[4] M. A. Novak,[5] and W. C. Nunes[5]

$$M = N\mu\,\mathrm{L}\left(\frac{\mu H}{kT}\right) \longrightarrow M = N\mu\,\mathrm{L}\left(\frac{\mu H}{k(T+T^*)}\right)$$

$$kT^* = \varepsilon_D$$

$$\varepsilon_D = \alpha\mu^2/d^3$$

$$T^* = \frac{\alpha}{k}\frac{\mu^2}{d^3} = \frac{\alpha}{k}N\mu^2 = \frac{\alpha}{k}\frac{M_S^2}{N}$$

PHYSICAL REVIEW B, VOLUME 64, 144420

Granular Cu-Co alloys as interacting superparamagnets

Paolo Allia,[1] Marco Coisson,[2] Paola Tiberto,[3] Franco Vinai,[3] Marcelo Knobel,[4] M. A. Novak,[5] and W. C. Nunes[5]

$$M = N_a \mu_a \, \mathrm{L}\left(\frac{\mu_a H}{kT} \right) \quad \longrightarrow \quad M = N \mu \, \mathrm{L}\left(\frac{\mu H}{k(T + T^*)} \right)$$

$$\mu_a = \frac{1}{1 + \dfrac{T^*}{T}} \mu, \qquad N_a = \left(1 + \frac{T^*}{T} \right) N$$

$$\chi = \frac{N\mu^2}{3k(T+T^*)} \qquad \frac{1}{\chi} = 3kN\left(\frac{T}{M_S^2}\right) + 3\alpha$$

$$T^* = \frac{\alpha}{k}\frac{\mu^2}{d^3} = \frac{\alpha}{k}N\mu^2 = \frac{\alpha}{k}\frac{M_S^2}{N}$$

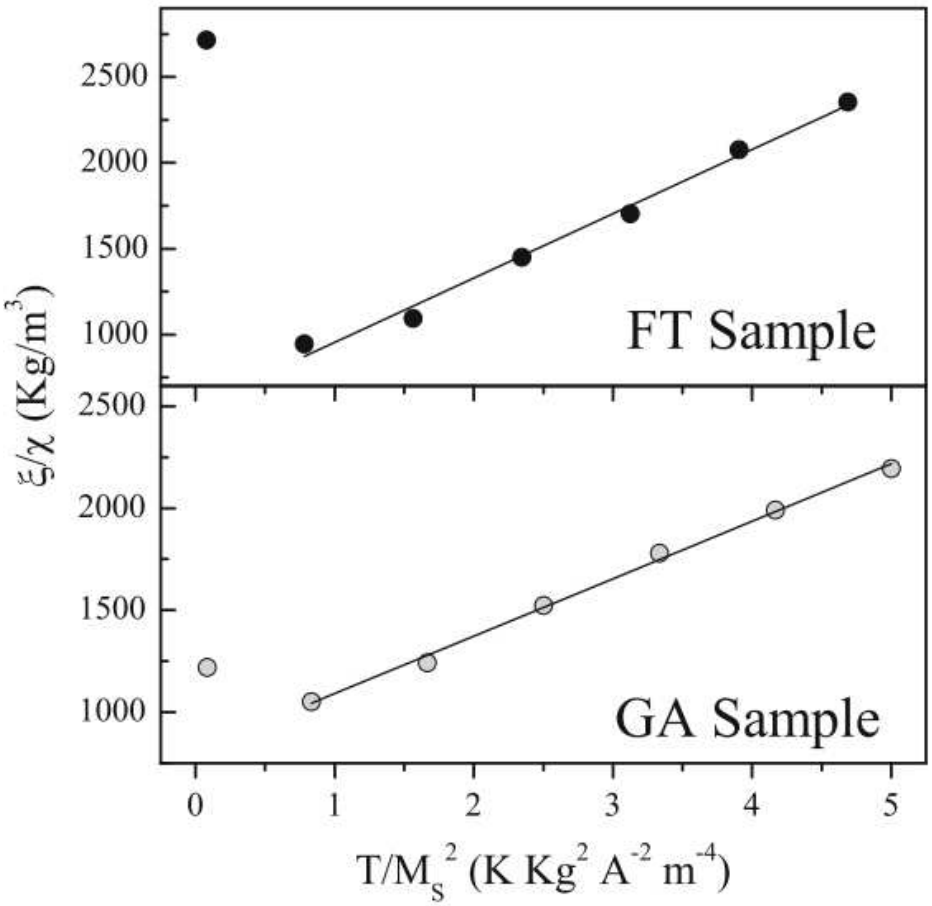
2500
2000
1500
1000
FT Sample
2500
2000
1500
1000
GA Sample
0
1
2
3
4
5
ξ/χ (Kg/m3)
T/MS2 (K Kg2 A-2 m-4)

$$M = N\sum_i p_i \mu_i \mathrm{L}\left(\frac{\mu_i H}{k(T+T^*)}\right) \quad \Longleftrightarrow \quad M = N_a \sum_i p_i \mu_{ai} \mathrm{L}\left(\frac{\mu_{ai} H}{kT}\right)$$

$$\mu_{ai} = \frac{1}{1+\frac{T^*}{T}}\mu_i \qquad \langle \mu_a \rangle = \frac{1}{1+\frac{T^*}{T}}\langle \mu \rangle$$

En el modelo de Allia, la proporcionalidad entre μ_a y μ es independiente de H.
Por lo tanto el modelo podría aplicarse a un ciclo de histéresis completo.
Sin embargo…

$$M = N\sum_i p_i \mu_i \mathrm{L}\left(\frac{\mu_i H}{k(T+T^*)}\right) \quad \Longleftrightarrow \quad M = N_a \sum_i p_i \mu_{ai} \mathrm{L}\left(\frac{\mu_{ai} H}{kT}\right)$$

$$\mu_{ai} = \frac{1}{1+\frac{T^*}{T}}\mu_i \qquad \langle \mu_a \rangle = \frac{1}{1+\frac{T^*}{T}}\langle \mu \rangle$$

$$\chi = \frac{M\sum_i p_i \mu_i^2}{3k(T+T^*)} = \frac{N\langle \mu^2 \rangle}{3k(T+T^*)}$$

$$\rho = \frac{\langle \mu^2 \rangle}{\langle \mu \rangle^2} \equiv \frac{\langle \mu_a^2 \rangle}{\langle \mu_a \rangle^2}$$

$$\frac{\rho}{\chi} = 3kN\left(\frac{T}{M_S^2}\right) + 3\alpha$$

J Nanopart Res (2011) 13:7277–7293
DOI 10.1007/s11051-011-0642-2

RESEARCH PAPER

Dynamic effects of dipolar interactions on the magnetic behavior of magnetite nanoparticles

Paolo Allia · Paola Tiberto

PEG5, PEG10, PEG90

0.15, 0.3, 2.7 wt%

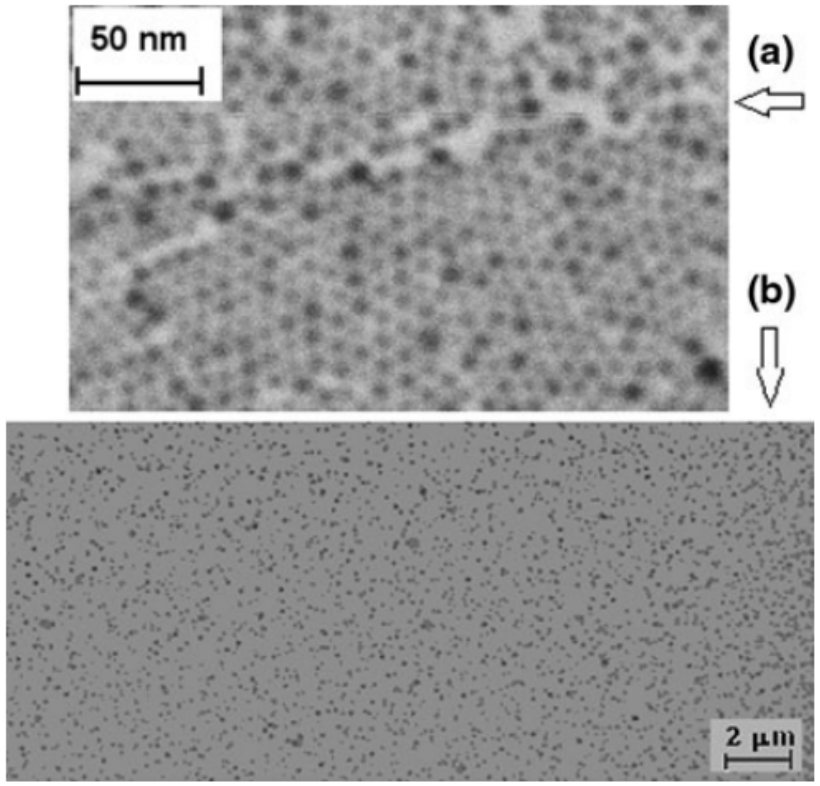

Fig. 1 **a** Contrast-enhanced Scanning Electron Micrograph of iron oxide NPs capped with oleic acid; **b** SEM image of PEGDA90 polymeric dispersion

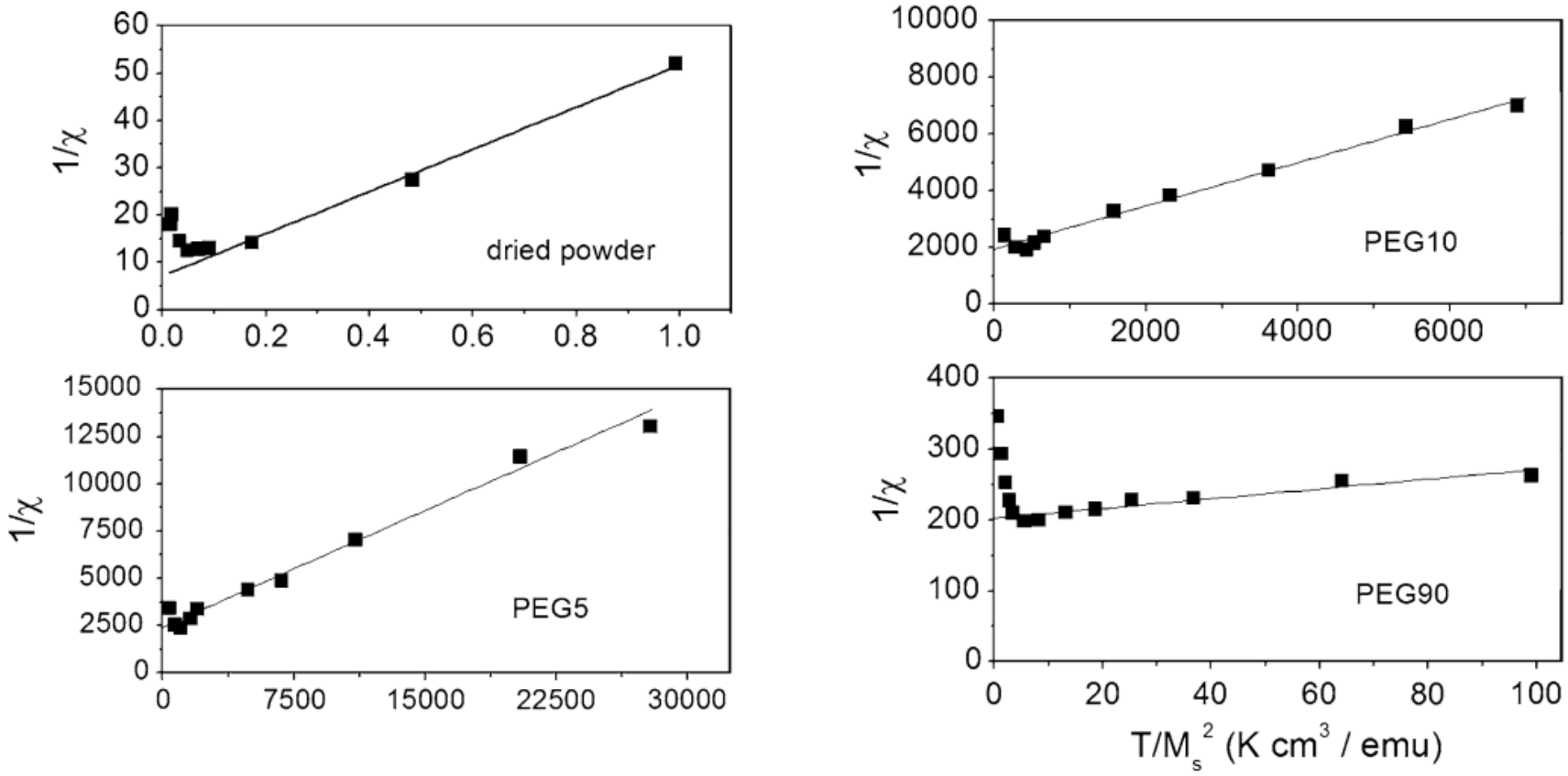

Fig. 4 Inverse susceptibility plotted as a function of the quantity T/M_s^2 for all studied samples. *Straight lines* are fits to high-temperature data

PHYSICAL REVIEW B **95**, 134421 (2017)

Dipolar interaction and demagnetizing effects in magnetic nanoparticle dispersions: Introducing the mean-field interacting superparamagnet model

F. H. Sánchez,[1,*] P. Mendoza Zélis,[1,2] M. L. Arciniegas,[1] G. A. Pasquevich,[1,2] and M. B. Fernández van Raap[1]

$$\vec{H}^E = \vec{H}^A + \vec{H}^D$$

Efectivo = **A**plicado + **D**ipolar

$$\kappa_u = \frac{\partial M_u}{\partial H_u^A}\Big|_{H_u^A=0}$$

Susceptibilidad aparente

$$\chi_u = \frac{\partial M_u}{\partial H_u^E}\Big|_{H_u^E=0}$$

Susceptibilidad real

$$\kappa_u = \chi_u/(1 + N_{su}\chi_u)$$

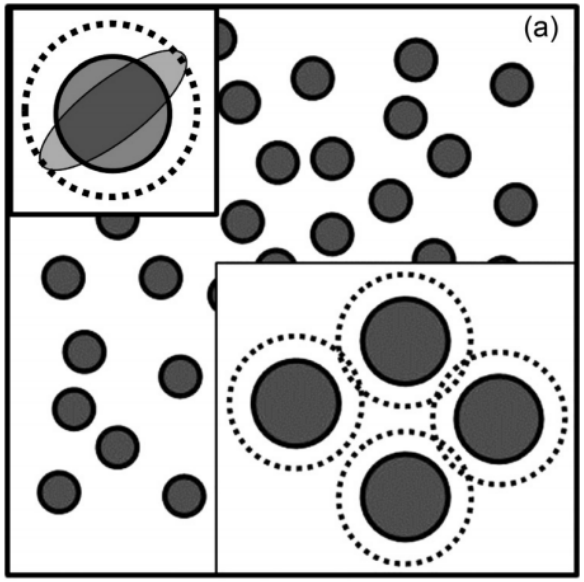

sphere of diameter D

mean near-neighbor distance $d = \gamma D$

$d_c = \gamma_c D_c$

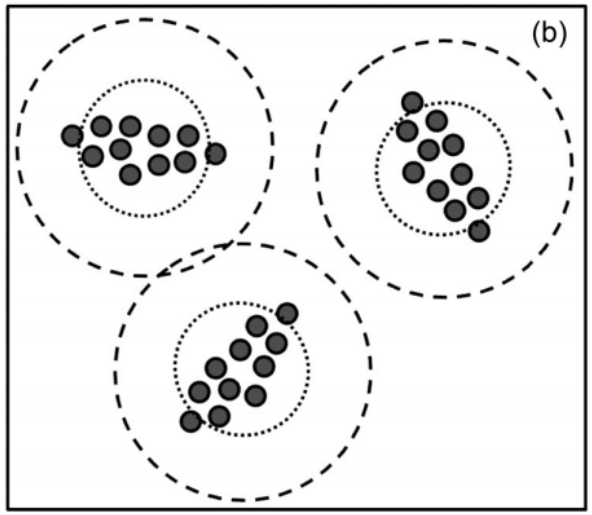

FIG. 2. Sketch of nanoparticles and clusters. (a) Left-top inset: NP shape (ellipse), sphere of diameter D with same volume V as NP (continuous contour), and sphere with diameter equal to mean near-neighbor distance $d = \gamma D$ (dotted contour, see also right-bottom inset). Main figure: random distribution of NPs in a nonmagnetic matrix. Packing fraction of dotted spheres is φ. (b) Nonrandom distribution of NPs. Dotted spheres of diameter D_c have same volume V_c as clusters. Mean distance between near-neighbor clusters is $d_c = \gamma_c D_c$. Dashed spheres diameter is d_c. Packing fraction of dashed spheres is φ_c.

Dipolar field at the position of NP i generated by the other NPs (j) is a function of moments $\vec{\mu}_j = \mu \hat{v}_j$, and vectors $\vec{d}_{ij} = d_{ij}\hat{u}_{ij}$, which are the positions of NPs j relative to NP i, where $\hat{v}_j$ and $\hat{u}_{ij}$ are unitary vectors, and is given by

$$\vec{H}_i^D = \frac{\mu}{4\pi} \sum_{j \neq i}^{n_{ps}} \vec{s}_{ij}/d_{ij}^3,$$

$$\vec{s}_{ij} = 3(\hat{v}_j \cdot \hat{u}_{ij})\hat{u}_{ij} - \hat{v_j}$$

Ecuación valida estrictamente para partículas esféricas, que generan un campo magnético disperso idéntico al de un dipolo de intensidad μ = V Ms. Sin embargo para partículas no estrictamente esféricas para:

$$d_{ij} > nD, \text{ with } n \text{ of the order of unity}$$

$$\vec{H}_i^D = \vec{H}_{i,I}^D + \vec{H}_{i,Q\neq I}^D$$

$$= \frac{\mu}{4\pi} \sum_{j\neq i}^{n_{pc}} \frac{\vec{s}_{ij}^{II}}{\left(d_{ij}^{II}\right)^3} + \frac{\mu}{4\pi} \sum_{Q\neq I}^{n_{cs}} \sum_{j=1}^{n_{pc}} \frac{\vec{s}_{ij}^{IQ}}{\left(d_{ij}^{IQ}\right)^3}$$

$$d_{ij}^{IQ} \longrightarrow d_{IQ}$$

Evaluamos el error introducido en el caso más desfavorable que es el de clusters primeros vecinos

$$\delta = |\langle 1/d_{ij}^3 \rangle - 1/d_c^3| / (1/d_c^3)$$

$$\delta = |\langle 1/d_{ij}^3 \rangle - 1/d_c^3| / (1/d_c^3)$$

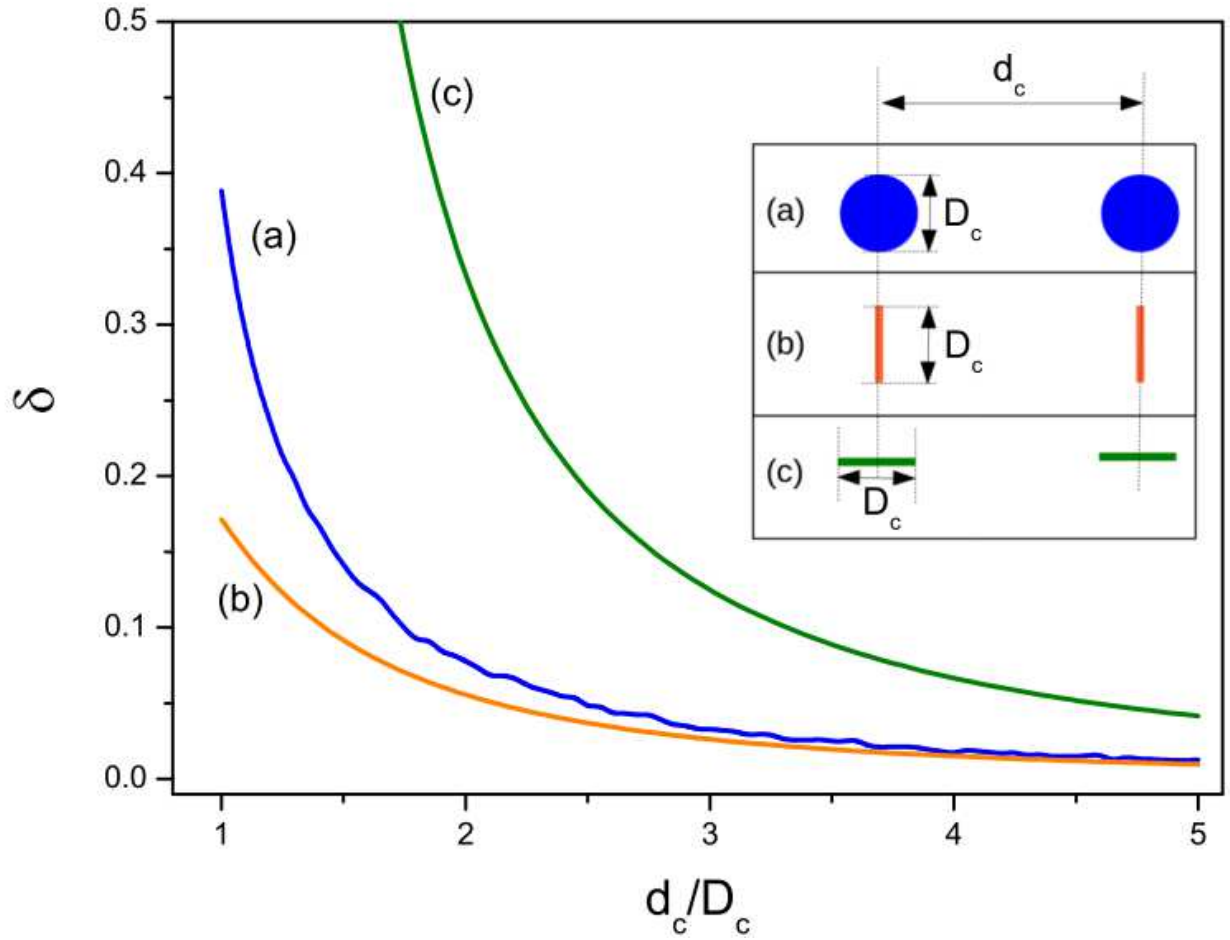

Now, we define the nondimensional quantities:

$$\vec{\lambda}_i = \frac{d^3}{n_{pc}-1} \sum_{j \neq i}^{n_{pc}} \frac{\vec{s}_{ij}^{II}}{\left(d_{ij}^{II}\right)^3} \quad \text{and}$$

$$\vec{\lambda}_{ci} = \frac{d_c^3}{n_{ps}-n_{pc}} \sum_{Q \neq I}^{n_{cs}} \frac{1}{d_{IQ}^3} \sum_{j=1}^{n_{pc}} \vec{s}_{ij}^{IQ}.$$

$\vec{\lambda}_i$ and $\vec{\lambda}_{ci}$ are invariant under similarity transformations

$$\vec{H}_{i,I}^{D} = \frac{\mu}{4\pi} \frac{n_{pc}-1}{\gamma^3 D^3} \vec{\lambda}_i,$$

$$\vec{H}_{i,Q \neq I}^{D} = \frac{\mu}{4\pi} \frac{n_{ps}-n_{pc}}{\gamma_c^3 D_c^3} \vec{\lambda}_{ci}.$$

Averaging over the specimen and considering the special case where the specimen magnetization $\vec{M}_s$ lays along one principal direction

$$\begin{aligned}\vec{H}^D &= \langle \vec{H}_i^D \rangle = \vec{H}_{c,\text{int}}^D + \vec{H}_{c,\text{ext}}^D \\ &= \frac{1}{24}\left(\frac{n_{pc}-1}{\gamma^3}\vec{\lambda} + \frac{(n_{cs}-1)\varphi}{\gamma^3\gamma_c^3}\vec{\lambda}_c\right) M^S \\ &= -N_{su}^E \vec{M}_s, \end{aligned} \tag{6}$$

where $\vec{H}_{c,\text{int}}^D = \langle \vec{H}_{i,I}^D \rangle$ and $\vec{H}_{c,\text{ext}}^D = \langle \vec{H}_{i,Q\neq I}^D \rangle$

$$\mu = V M^S$$

$$\langle \vec{\lambda}_i \rangle = \vec{\lambda}, \langle \vec{\lambda}_{ci} \rangle = \vec{\lambda}_c$$

Magnetización por unidad de volumen de “cluster” y de “specimen”

$$M_c = \frac{\varphi}{\gamma^3} M \quad \text{and} \quad M_s = x_V M = \frac{\varphi \varphi_c}{\gamma^3 \gamma_c^3} M$$

$$\vec{H}^D_{c,\text{int}} = -N_{cu} \vec{M}_c .$$

$$\vec{H}^D_{c,\text{ext}} = -(N_{su} \vec{M}_s - N_{cu} \vec{M}_s).$$

$$\vec{\lambda} = -24\frac{\varphi}{n_{pc}-1}N_{cu}\frac{\vec{M}}{M^S},$$

$$\vec{\lambda}_c = -24\frac{\varphi\varphi_c}{n_{cs}-1}(N_{su}-N_{cu})\frac{\vec{M}}{M^S},$$

$$N_u^E = \frac{\varphi}{\gamma^3}\left(N_{cu}\left(1 - \frac{\varphi_c}{\gamma_c^3}\right) + N_{su}\frac{\varphi_c}{\gamma_c^3}\right),$$

$$N_{su}^E = \left(\frac{\gamma_c^3}{\varphi_c} - 1\right)N_{cu} + N_{su}.$$

Note that $N_u^E = x_V N_{su}^E$.

Calculo de Neff

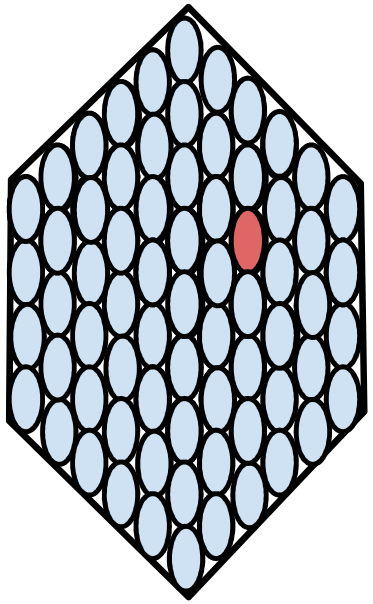

Muestra en cuyo interior hay cluster con forma de elipse de color celeste.

Calculamos el campo demagnetizante que actúa en promedio sobre las partículas que componen la dispersión.

Lo calculamos dentro de un cluster (y no en cualquier sitio) por la razon obvia que las partículas sólo estarán dentro de los clusters.

Entonces, la propuesta es calcular el campo demagnetizante en el interior del cluster rojo.

El campo dentro del cluster rojo lo planteamos como la suma de las contribuciones del propio cluster en cuestión por un lado + todo el resto de la muestra (sin ese cluster):

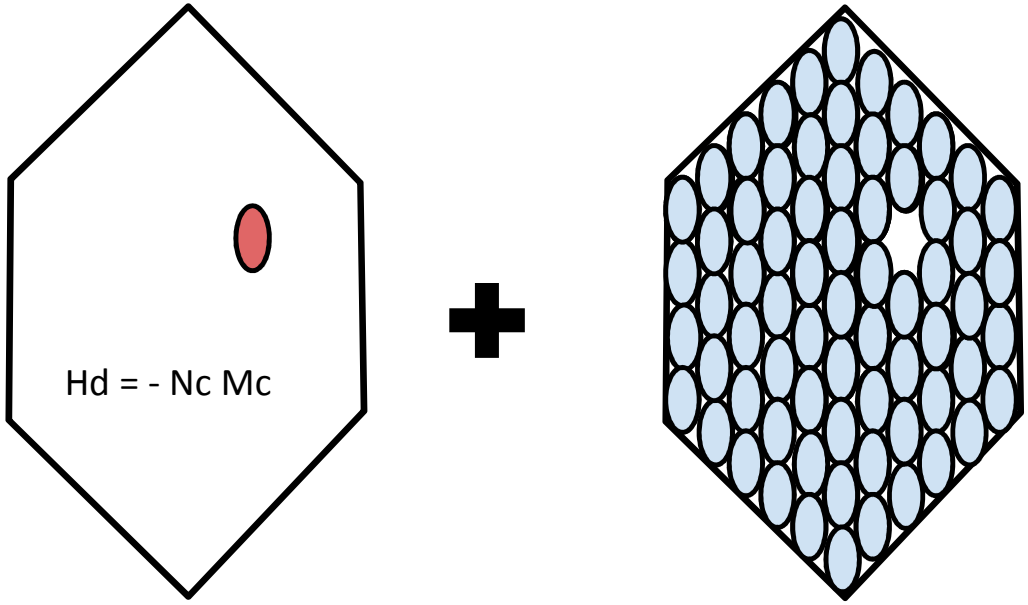

El campo demagnetizante debido al cluster rojo es Hd = - Nc Mc donde Mc es la magnetización media dentro de un cluster. Se cumple que Mc = ϕ/γ^3 M, donde M es la magnetizacion media de partícula (su momento medio dividido su volumen) y Mc es el momento total dentro del cluster dividido el volumen del cluster).

Ahora calculamos el campo demagnetizante debido al resto de la muestra sin ese cluster. Esa contribución la podemos calcular aproximándola por la resta entre el campo demagnetizante de una muestra continua magnetizada con magnetización de espécimen Ms = (ϕ/γ^3) (ϕ_c/γ_c^3) M menos la de un cluster en la posición del rojo con magnetización también Ms:

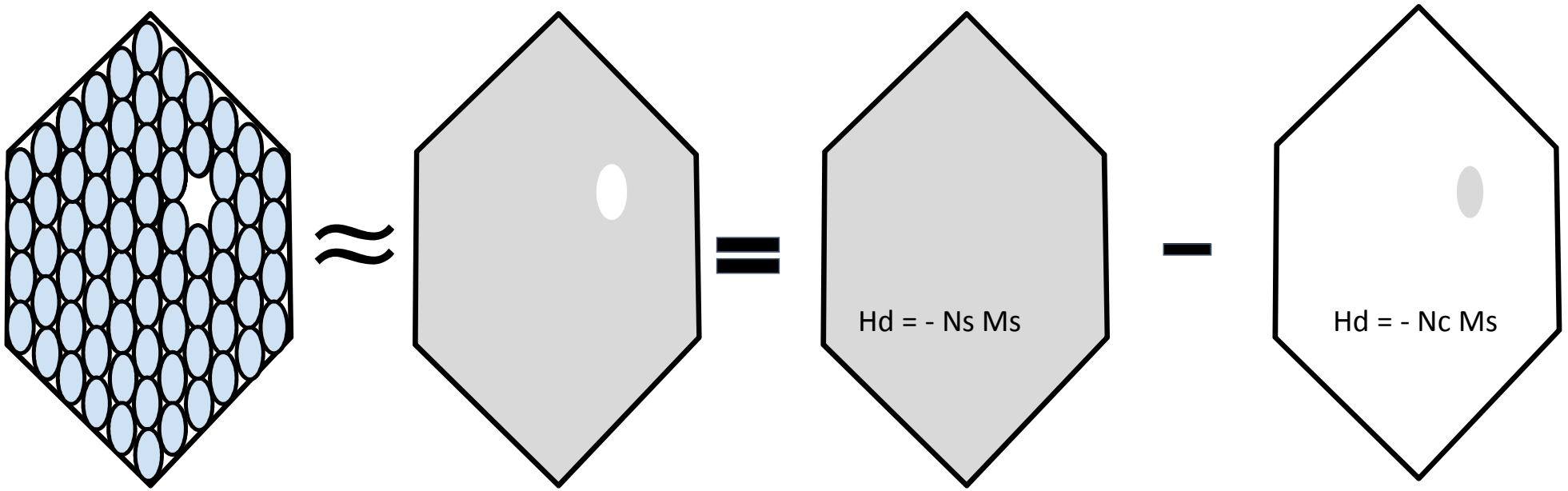

El campo demagnetizante seria Hd = - Ns Ms - (- Nc Ms) = -Ns Ms + Nc Ms

Entonces:

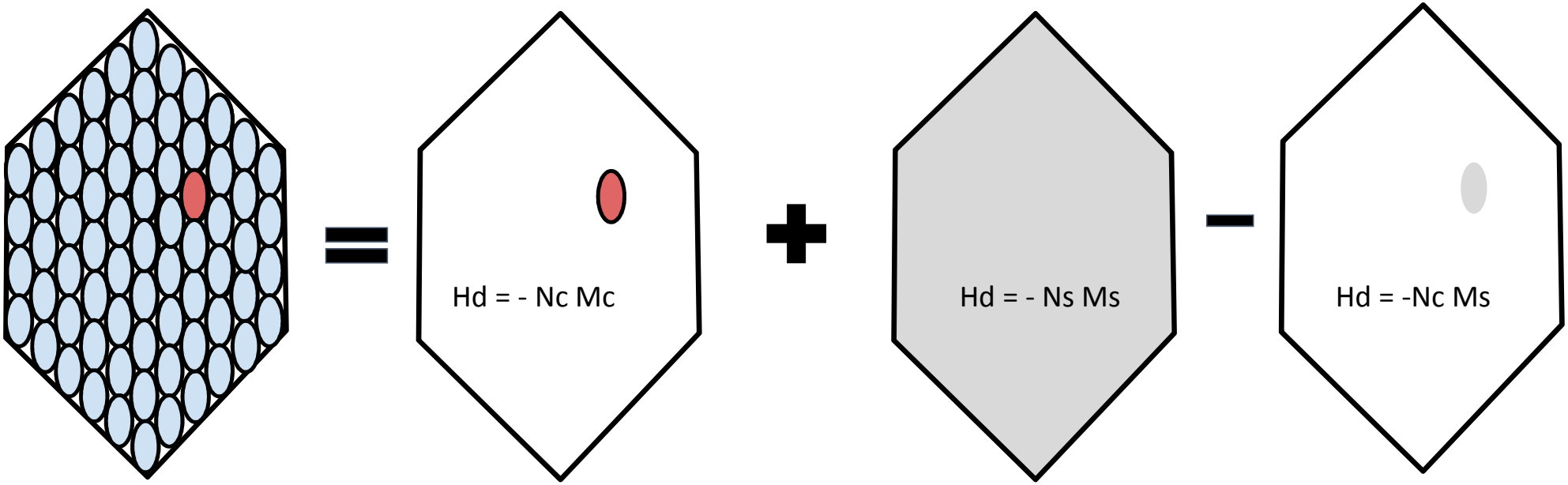

El campo demagnetizante sería Hd = (-Nc Mc) + (-Ns Ms) - (- Nc Ms)
Reagrupando: Hd = - Ns Ms - Nc (Ms-Mc)
Recordando que Ms = (ϕ/γ^3) (ϕ_c/γ_c^3) M y que Mc = (ϕ/γ^3) M podemos llegar a:

$$Hd = -\{ (\phi/\gamma^3) [Ns + Nc (1- \phi_c/\gamma_c^3)] \} M$$

$$N_u^E = \frac{\varphi}{\gamma^3}\left(N_{cu}\left(1 - \frac{\varphi_c}{\gamma_c^3}\right) + N_{su}\frac{\varphi_c}{\gamma_c^3}\right),$$

$\gamma_c \to \infty$ ➡ $N_u^E = \frac{\varphi}{\gamma^3} N_{cu}$

$\gamma_c = 1$ and $\varphi_c = 1$ ➡ $N_u^E = \frac{\varphi}{\gamma} N_{su} = x_V N_{su}$

$\gamma \to \infty$ ➡ $H^D = -N_u^E M = N_{su}^E M_s$ tends to zero

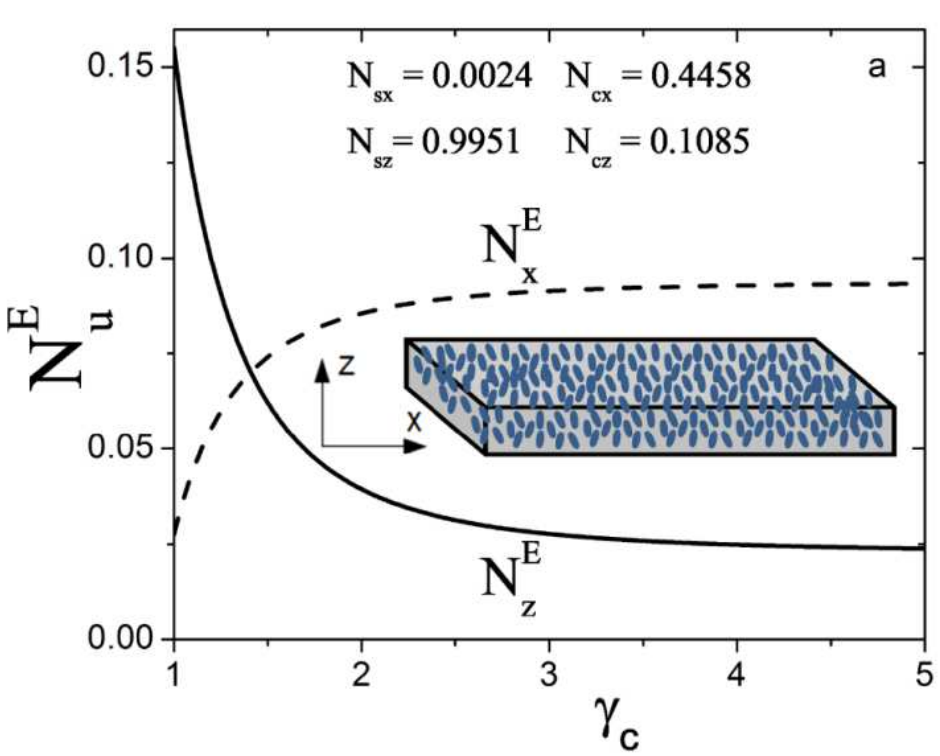
a
$N_{sx} = 0.0024$ $N_{cx} = 0.4458$
$N_{sz} = 0.9951$ $N_{cz} = 0.1085$
N_x^E
N_z^E
N_u^E
γ_c
z
x
0.15
0.10
0.05
0.00
1
2
3
4
5

(a)

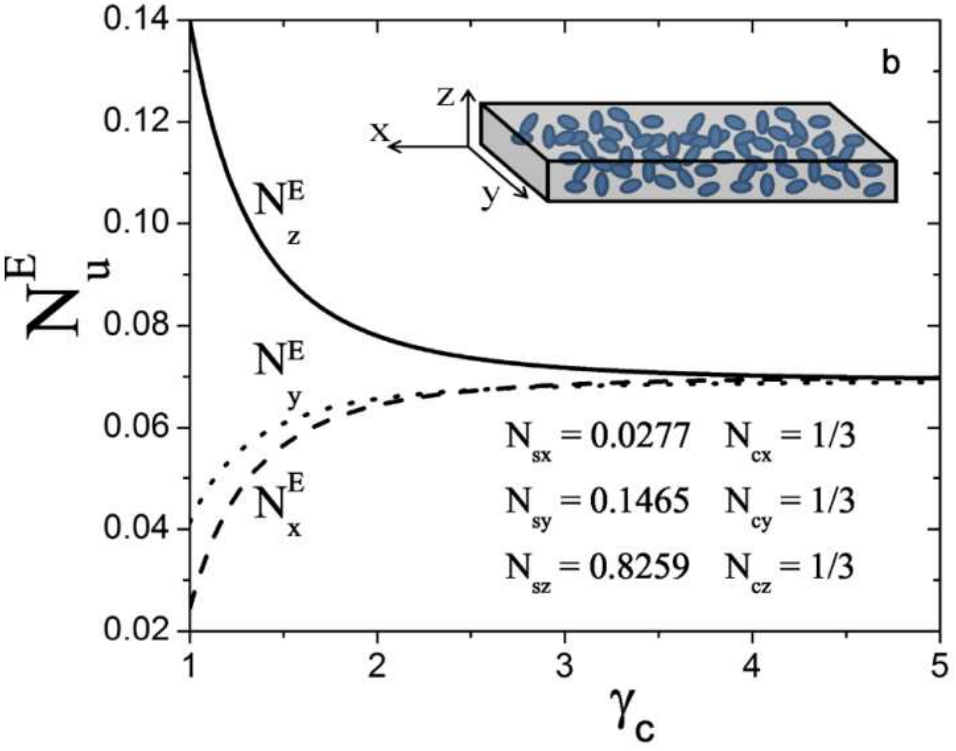
b
N_z^E
N_y^E
N_x^E
$N_{sx} = 0.0277$ $N_{cx} = 1/3$
$N_{sy} = 0.1465$ $N_{cy} = 1/3$
$N_{sz} = 0.8259$ $N_{cz} = 1/3$
N_u^E
γ_c
z
x
y
0.14
0.12
0.10
0.08
0.06
0.04
0.02
1
2
3
4
5

(b)

$$M_u\left(H_u^A, T\right) = \frac{1}{V}\int \mu F\left(\frac{\mu_0\mu\left(H_u^A - N_u^E M_u\right)}{kT}\right) f(\mu) d\mu.$$

$$M_u\left(H_u^A, T\right) \approx \frac{1}{V_a}\int \mu_a F\left(\frac{\mu_0\mu_a H_u^A}{kT}\right) g(\mu_a) d\mu_a$$

$$\mu_a \approx \mu\left(1 - N_u^E M_u / H_u^A\right)$$

En general, g y f pueden tener diferente forma matemática, y μ_a es una función multivaluada de μ.
Sin embargo, a campos suficientemente bajos en donde la susceptibilidad se mantiene constante:

$$g(\mu_a) = \frac{\chi_u}{\kappa_u} f\left(\frac{\chi_u}{\kappa_u}\mu_a\right)$$

$$\chi_u = \kappa_u/(1 - N_u^E \kappa_u)$$

En estas condiciones, μ_a es una función univaluada de μ ; además g y f tendrán la misma forma matemática.

$$1/\kappa_u = 1/\chi_u + N_u^E$$

$$\frac{1}{\kappa_u} = \frac{k}{\mu_0 V}\left(\frac{T}{\zeta_u(\nu) M^{S^2}}\right) + N_u^E,$$

$$\chi_{u0}(\nu,\theta) = 3\zeta_u(\nu,\theta)\chi_L,$$

$$1/\kappa_u = 1/\chi_u + N_u^E$$

$$\frac{1}{\kappa_u} = \frac{3k}{\mu_0 \langle V \rangle} \left(\frac{T}{\rho M^{s^2}} \right) + N_u^E$$

$$\varepsilon_u = -\mu_0 \langle \vec{\mu}_i \cdot \vec{H}_i \rangle = \mu_0 N_u^E {M_u}^2 \langle V \rangle,$$

J Nanopart Res (2011) 13:7277–7293
DOI 10.1007/s11051-011-0642-2

RESEARCH PAPER

PEG5, PEG10, PEG90

0.15, 0.3, 2.7 wt%

Dynamic effects of dipolar interactions on the magnetic behavior of magnetite nanoparticles

Paolo Allia · Paola Tiberto

TABLE I. Values of NP volume fraction (x_V) calculated from data reported in Ref. [12], NP diameter reported in Ref. [40] (D') and obtained in the present work (D), mean interparticle distances reported in Ref. [12] (d') and obtained in the present work (d), effective demagnetizing factor (N_u^E), and relative distances γ and γ_c.

Specimen	x_V	D' (nm)	D (nm)	d' (nm)	d (nm)	N_u^E	γ	γ_c
Dried Powder (DP)	0.046(5)	9.8	9.2(3)	20	17(1)	0.031(5)	1.9(1)	1.2(1)
PEG5	$2.7(3) \times 10^{-4}$	8.2	8.2(3)	16	13(1)	0.054(7)	1.6(1)	7.4(4)
PEG10	$5.5(5) \times 10^{-4}$	8.2	8.3(3)	14	12(1)	0.09(1)	1.4(1)	6.9(3)
PEG90	0.0046(5)	–	17(2)	29	25(3)	0.073(4)	1.5(1)	3.2(1)

J Nanopart Res (2011) 13:7277–7293
DOI 10.1007/s11051-011-0642-2

RESEARCH PAPER

PEG5, PEG10, PEG90

0.15, 0.3, 2.7 wt%

Dynamic effects of dipolar interactions on the magnetic behavior of magnetite nanoparticles

Paolo Allia · Paola Tiberto

$D_c \approx 40$ nm in PEG90

$d_c = \gamma_c D_c \approx 130$ nm

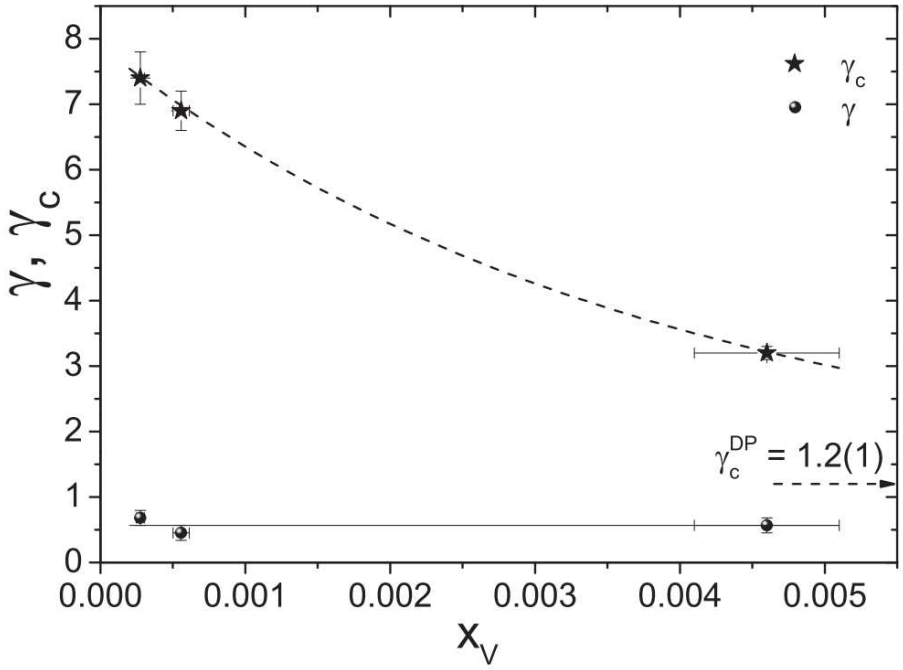

B. Study of hydrogel (PVA) and magnetic nanoparticles Fe_3O_4 ferrogels

TABLE II. Specimens FGXPi (see text), NPs volume fractions x_V, rectangular prism dimensions l_x, l_y, and l_z, and specimen shape demagnetizing factors (calculated according to Ref. [42])

Specimen	x_V	l_x(mm)	l_y(mm)	l_z(mm)	N_{sx}	N_{sy}	N_{sz}
FG1P3	0.0017(1)	4.00(2)	2.00(2)	0.12(2)	0.036(4)	0.074(9)	0.89(1)
FG3P7	0.0067(4)	4.68(2)	1.32(2)	0.24(2)	0.046(3)	0.17(1)	0.78(1)
FG6P6	0.0158(8)	4.90(2)	1.10(2)	0.20(2)	0.037(3)	0.17(1)	0.79(1)
FG9aP1	0.0169(9)	4.00(2)	2.00(2)	0.14(2)	0.040(4)	0.083(9)	0.88(1)
FG9aP5		4.90(2)	1.00(2)	0.14(2)	0.028(4)	0.15(1)	0.83(2)
FG9bP2	0.020(1)	3.90(2)	3.00(2)	0.24(2)	0.066(3)	0.087(5)	0.847(9)
FG9bP4		5.00(2)	1.00(2)	0.24(2)	0.040(2)	0.21(1)	0.75(1)

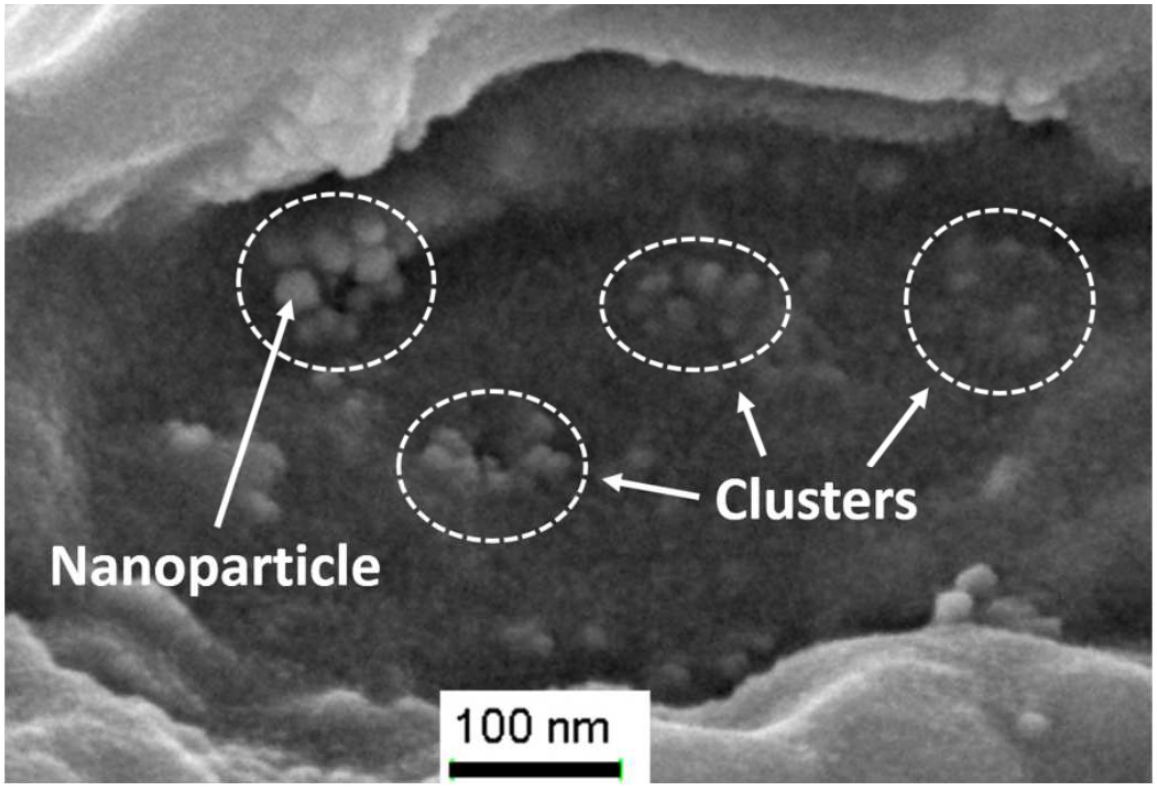

FIG. 8. FESEM image of FG6 specimen. Clusters of NPs are indicated.

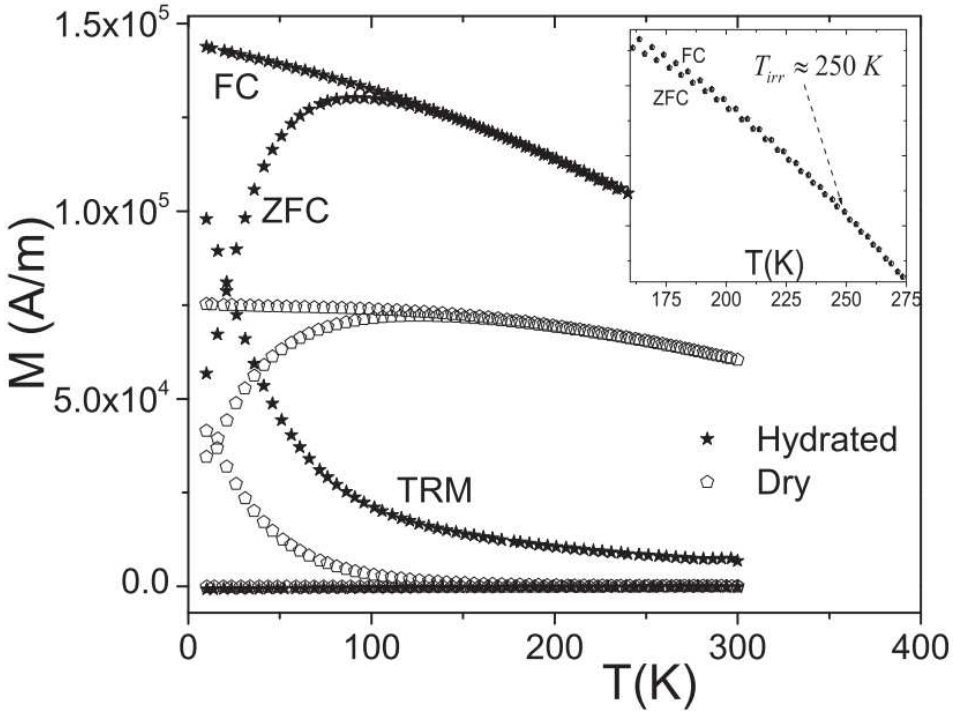

FIG. 9. ZFC-FC-TRM curves from FG9aP1 specimen. Cooling part of ZFC and TRM measurements were performed under zero field. Warming part of ZFC and FC measurements were performed under a 8 kA/m field. Field was applied parallel to the longest (l_x) prism dimension. Inset shows a close look of ZFC-FC around irreversible temperature (T_{irr}) of dry specimen

2. *Determination of NPs intrinsic properties*

$$\frac{1}{\kappa_u} = \frac{3k}{\mu_0 \langle V \rangle} \left(\frac{T}{\rho M^{S^2}} \right) + N_u^E$$

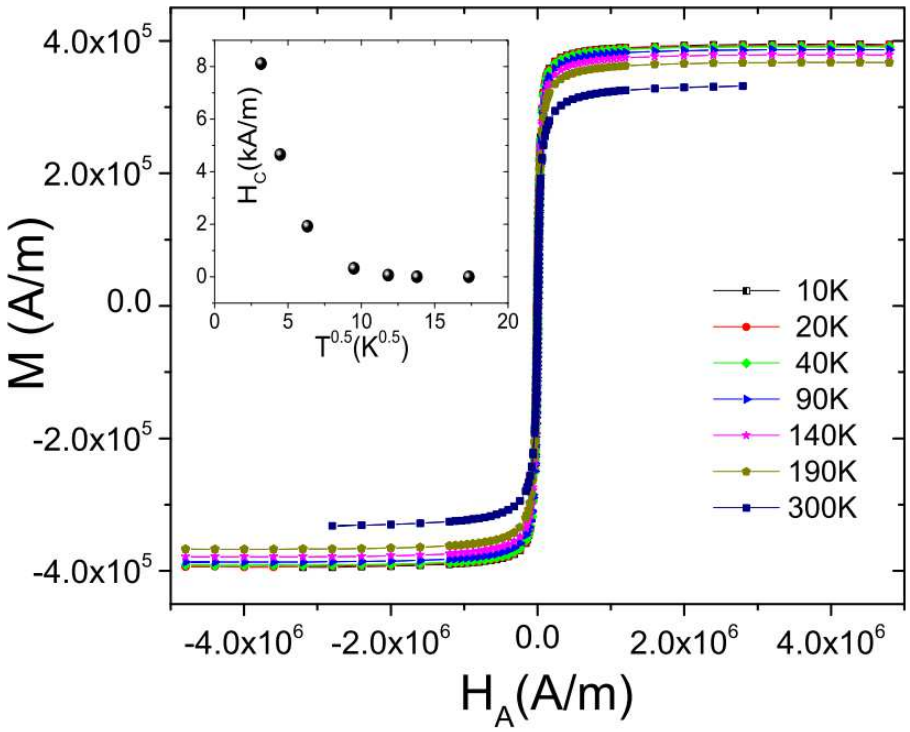

FIG. 10. $M(H^A)$ cycles for FG9P1 specimen at several temperatures. Field was applied parallel to the longest (l_x) prism dimension. Inset shows coercive field (H_c) vs. temperature.

$$M(H^A,T) \approx \frac{1}{\langle V_a \rangle} \int \mu_a L\left(\frac{\mu_0 \mu_a H^A}{kT}\right) g(\mu_a) d\mu_a$$

where we have used a Lognormal distribution as $g(\mu_a)$ and approximated $F \approx L$ disregarding, for the sake of simplicity, possible effects of finite values of $\nu = KV/kT$. Such

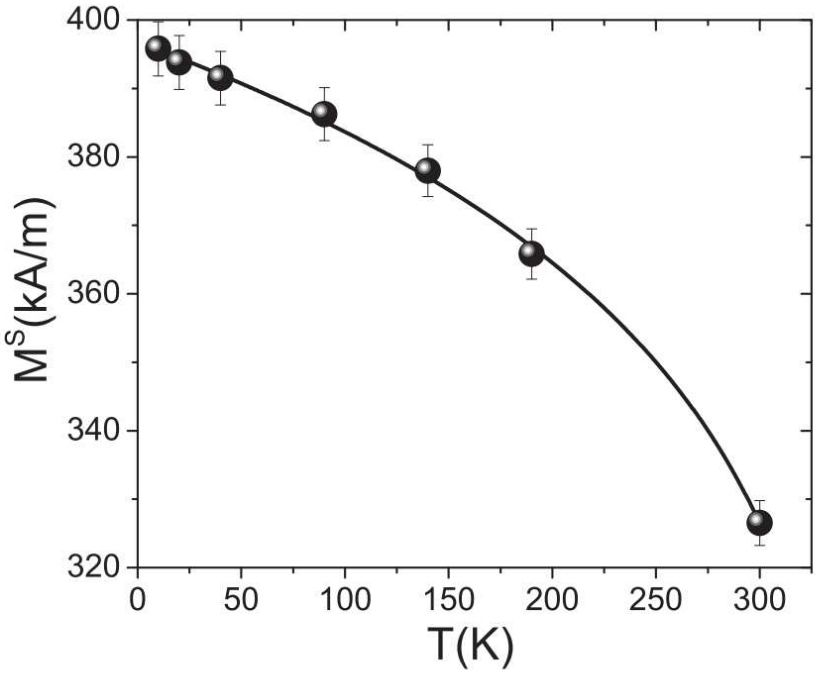

FIG. 11. Saturation magnetization M^S versus temperature T for FG9aP1 specimen. Dots were obtained from the analysis of Fig. 10 data. Line corresponds to fitting with $M^S(T) = A(1 - T/B)^C$. The values obtained were $A = 3.97(1) \times 10^2$ kA/m, $B = 350(8)$ K, and $C = 0.100(7)$

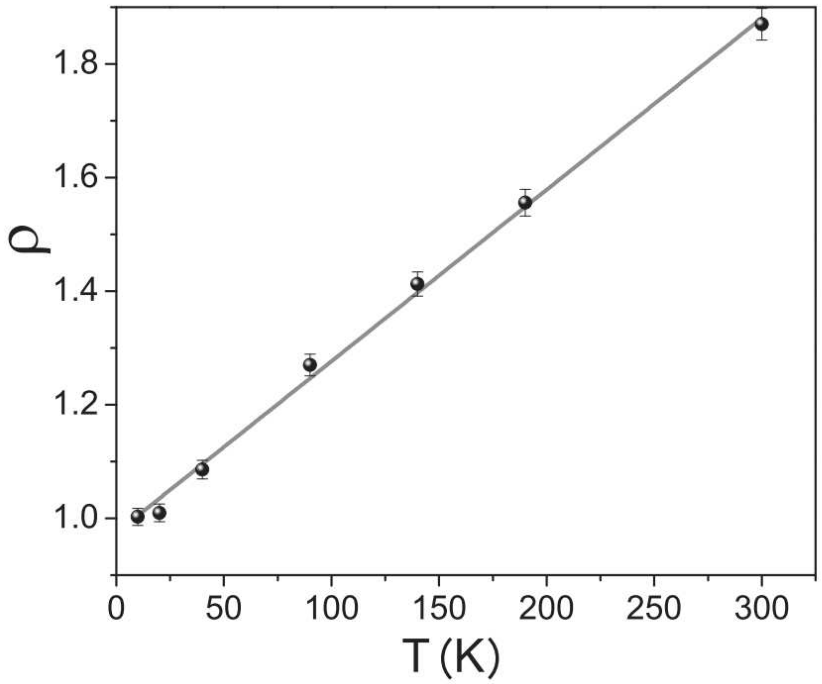

FIG. 12. $\rho = \langle\mu^2\rangle/\langle\mu\rangle^2$ versus temperature T were μ is the NP magnetic moment. Dots were obtained from the analysis of Fig. 10 data. Line corresponds to fitting with a linear function $\rho = AT + B$. The values obtained were $A = 3.1(1) \times 10^{-3}$ K^{-1} and $B = 0.97(1)$.

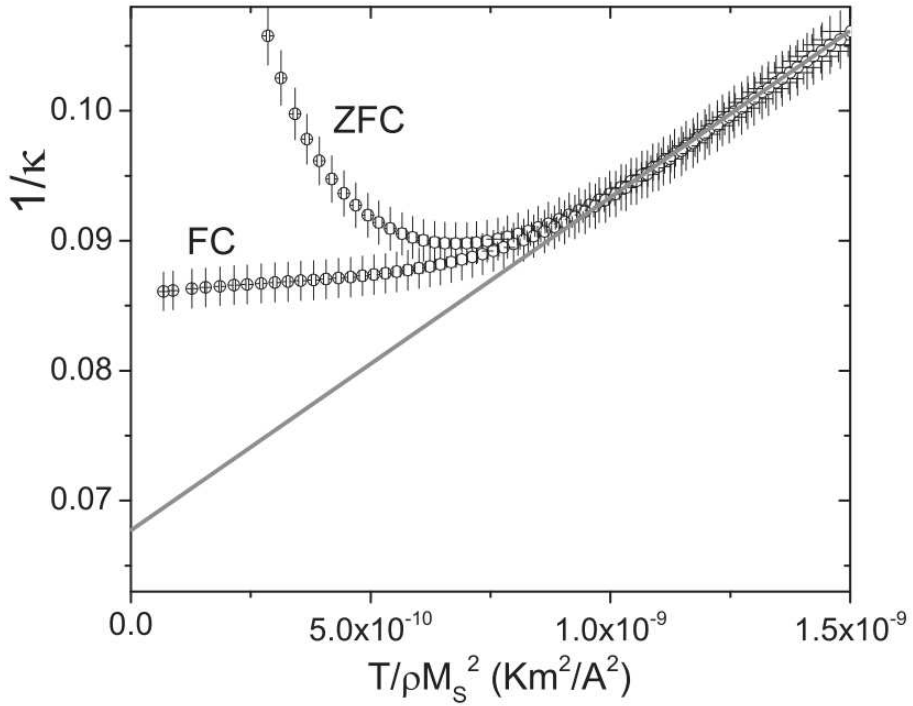

FIG. 13. Inverse of apparent susceptibility $1/\kappa_x$, obtained from ZFC and FC measurements, as a function of $T/\rho M^{S^2}$. Straight line is the fit of the linear region (specimen magnetization in thermal equilibrium).

$$\frac{1}{\kappa_u} = \frac{3k}{\mu_0 \langle V \rangle} \left(\frac{T}{\rho M^{S^2}} \right) + N_u^E$$

$$N_x^E = 0.068(1)$$

$$\langle V \rangle = 1.15(2) \times 10^3 \ \text{nm}^3$$

$$D = 13.0(1) \ \text{nm}$$

$$\chi_x = \frac{\kappa_x}{1 - N_x^E \kappa_x}$$

$$\chi_x \approx \chi_y \approx \chi_z$$

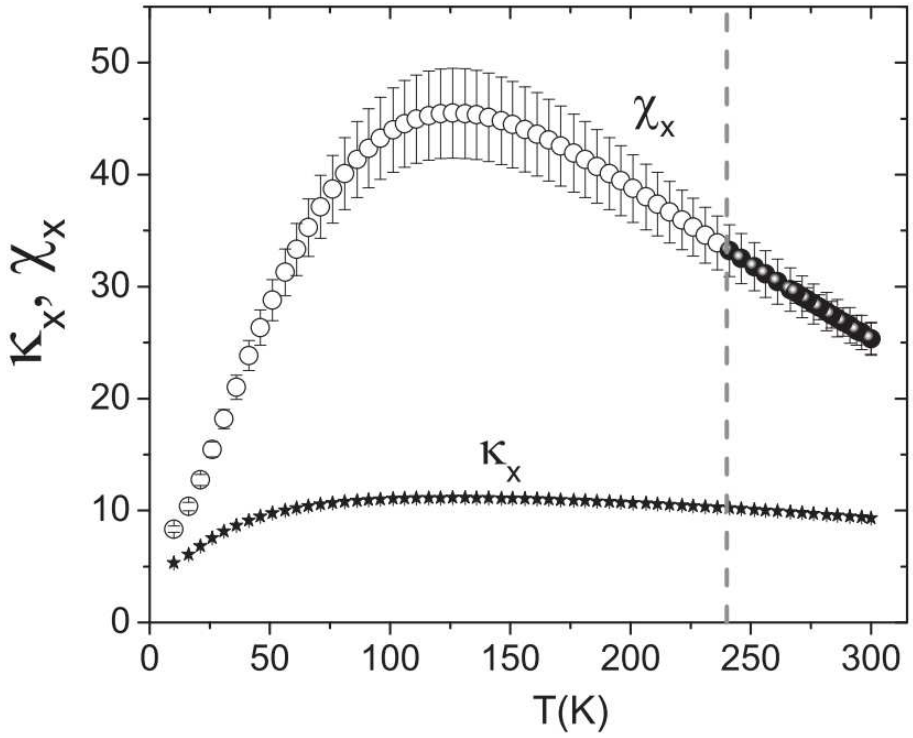

FIG. 14. Apparent susceptibility κ_x and corrected (true) susceptibility χ_x. Vertical dash line corresponds to $T = T_{\rm irr}$, therefore correction is only reliable at $T \geqslant T_{\rm irr}$ (black symbols for χ_x).

$$\mu_\chi = \left(\frac{\chi_u}{\kappa_u}\right)\mu_a$$

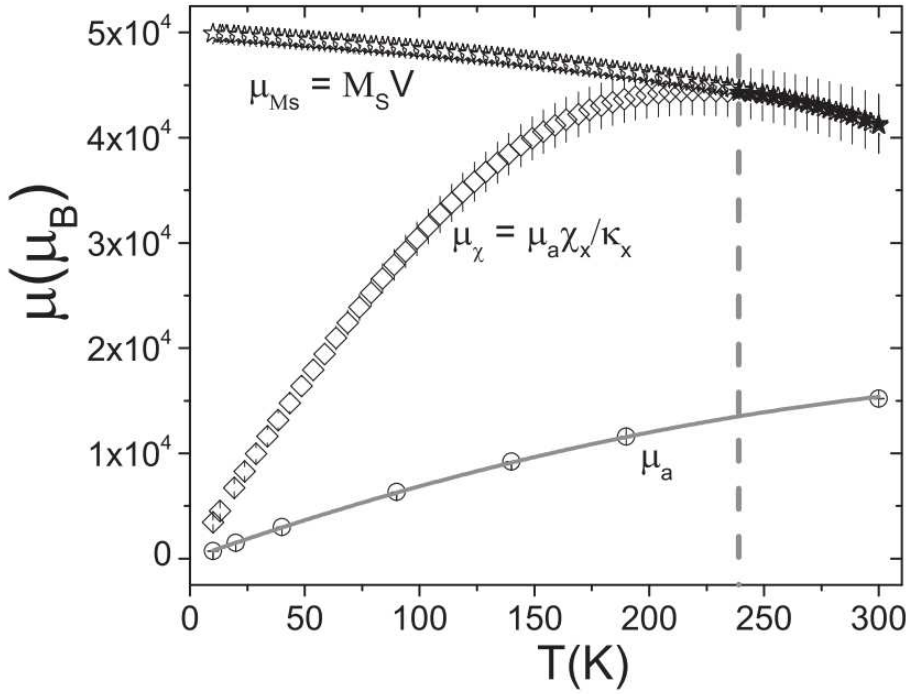

FIG. 15. NP magnetic moment μ: μ_a is the apparent NP moment, μ_χ is the corrected NP moment obtained with the present model, and μ_{Ms} is the NP moments obtained through saturation magnetization data. Vertical dash line corresponds to $T = T_{\text{irr}}$, therefore correction μ_χ is only reliable at $T \geqslant T_{\text{irr}}$ (black-star symbols).

3. *Parameters of NPs space distribution: Effective demagnetizing factor and demagnetizing factors of clusters*

$$\Phi_x > \Phi_y > \Phi_z$$

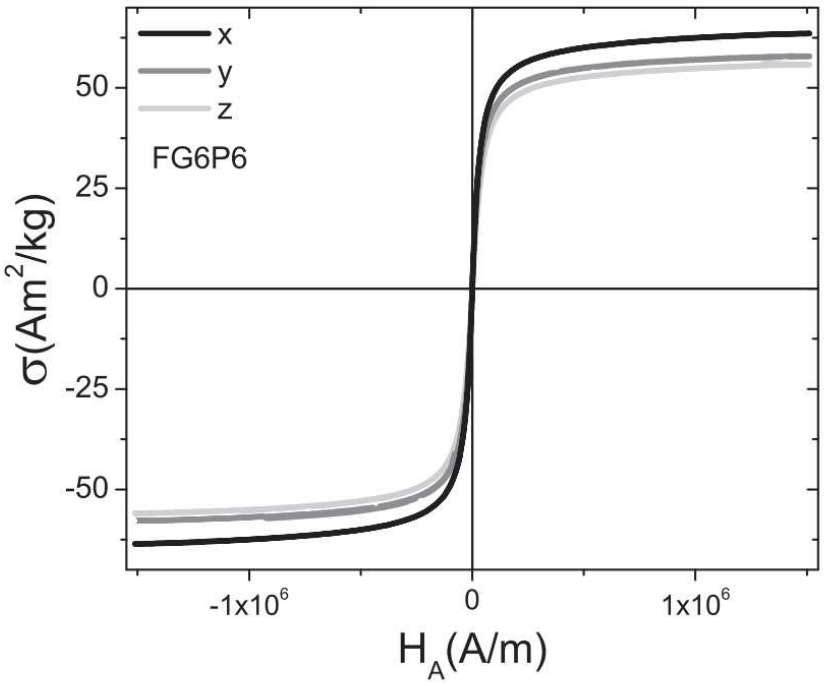

FIG. 16. $\sigma(H)$ cycles for specimen FG6P6 (raw data).

Specimen	x_V	l_x(mm)	l_y(mm)	l_z(mm)	N_{sx}	N_{sy}	N_{sz}
FG9aP1	0.0169(9)	4.00(2)	2.00(2)	0.14(2)	0.040(4)	0.083(9)	0.88(1)

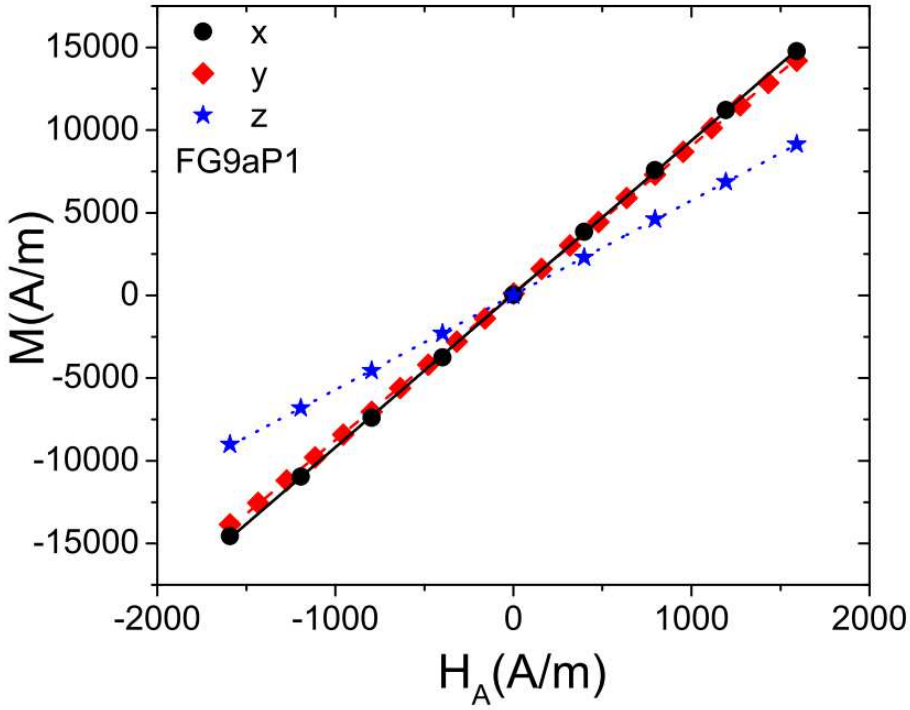

FIG. 17. Linear region of $M(H)$ curves, measured in FG9aP1 specimen with the applied field along the three prism directions. Curves were normalized at high fields as described in the text.

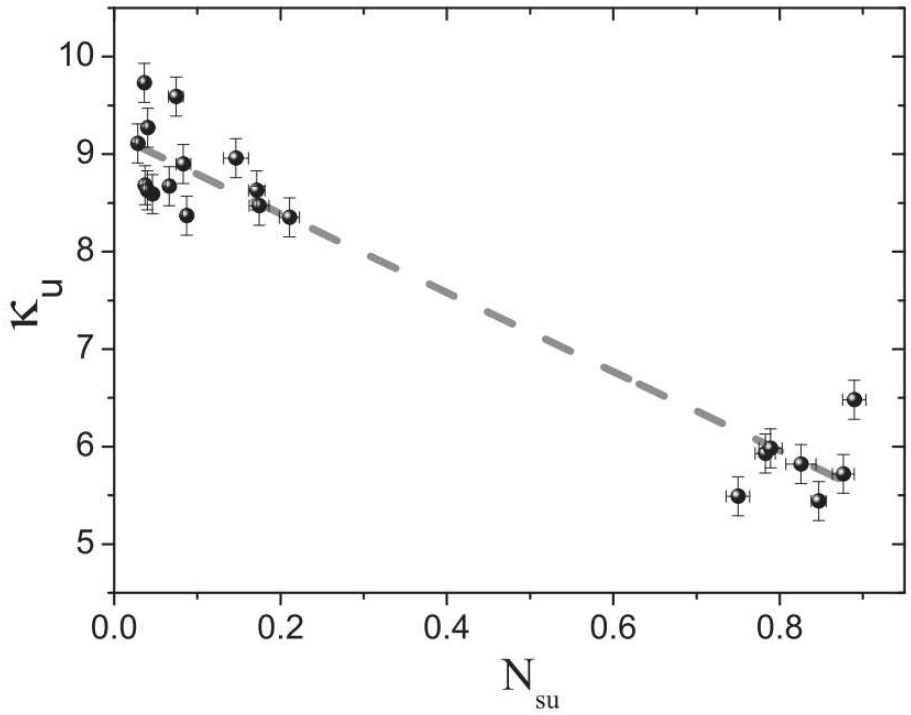

FIG. 18. Measured (apparent) susceptibilities κ_u versus demagnetizing factors N_{su} corresponding to specimen shape.

TABLE III. Susceptibilities κ_u measured in the three prism directions $u = x, y, z$. Relative distance parameters γ and γ_c. Specimen effective demagnetizing factors N^E_{su}. Demagnetizing factors N_{cu} associated to average cluster shape.

Specimen	κ_x	κ_y	κ_z	γ	γ_c	N^E_x	N^E_y	N^E_z	N_{cx}	N_{cy}	N_{cz}
FG1P3	9.7(2)	9.6(2)	6.5(2)	1.42(1)	4.6(2)	0.063(2)	0.065(2)	0.115(5)	0.26(1)	0.27(1)	0.47(2)
FG3P7	8.6(2)	8.6(2)	5.9(2)	1.35(1)	3.1(1)	0.077(3)	0.076(3)	0.129(6)	0.28(1)	0.28(1)	0.45(2)
FG6P6	8.7(2)	8.5(2)	6.0(2)	1.35(1)	2.32(8)	0.076(3)	0.079(3)	0.128(6)	0.29(1)	0.29(1)	0.44(2)
FG9aP1	9.3(2)	8.9(2)	5.7(2)	1.36(1)	2.25(8)	0.068(2)	0.073(3)	0.135(6)	0.27(1)	0.28(1)	0.48(2)
FG9aP5	9.1(2)	9.0(2)	5.8(2)	1.37(1)	2.25(8)	0.070(3)	0.072(3)	0.132(6)	0.28(1)	0.28(1)	0.47(2)
FG9bP2	8.7(2)	8.4(2)	5.4(2)	1.33(1)	2.19(7)	0.076(3)	0.080(3)	0.144(7)	0.27(1)	0.29(1)	0.47(2)
FG9bP4	8.6(2)	8.4(2)	5.5(2)	1.33(1)	2.18(7)	0.076(3)	0.080(3)	0.143(7)	0.28(1)	0.28(1)	0.47(2)

$$\kappa_u = \chi_u/(1 + N_{su}\chi_u) \qquad \chi_x \approx \chi_y \approx \chi_z \approx \chi \qquad \gamma^3\gamma_c^3 = \frac{\varphi\varphi_c}{x_V}$$

N^E_u, N_{cu}, γ, and γ_c are obtained

$$N^E_u = \frac{\varphi}{\gamma^3}\left(N_{cu}\left(1 - \frac{\varphi_c}{\gamma_c^3}\right) + N_{su}\frac{\varphi_c}{\gamma_c^3}\right), \qquad \mathrm{Tr}(N^E) = \frac{\varphi}{\gamma^3},$$

FESEM image shown in Fig. 8 correspond to FG6 sample and shows clusters of the order of 70 nm separated by distances of about 150–160 nm, consistently with results in Table III and Fig. 18 ($\gamma_c \approx 2.3$).

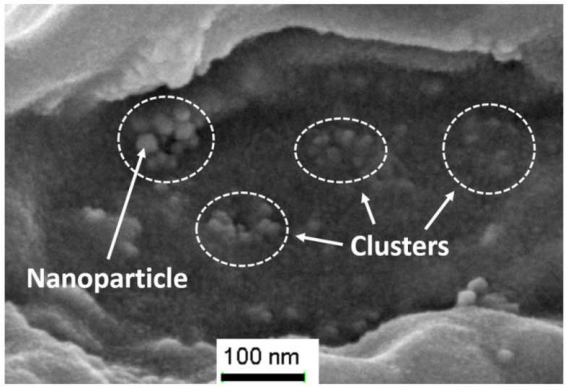

FIG. 8. FESEM image of FG6 specimen. Clusters of NPs are indicated.

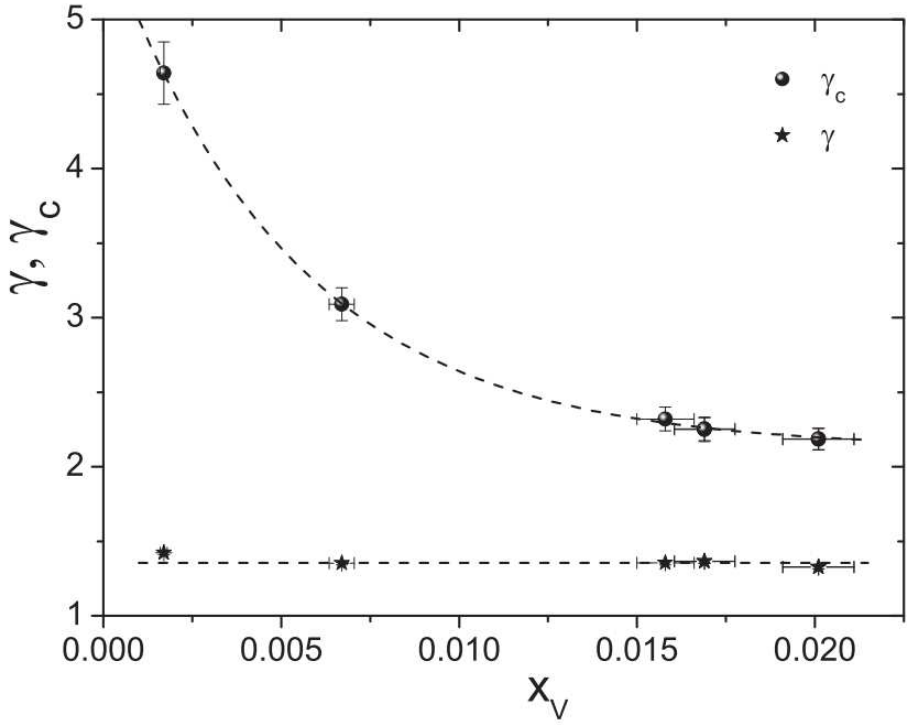

FIG. 19. Relative distance parameters γ and γ_c versus NPs volume fraction x_V.

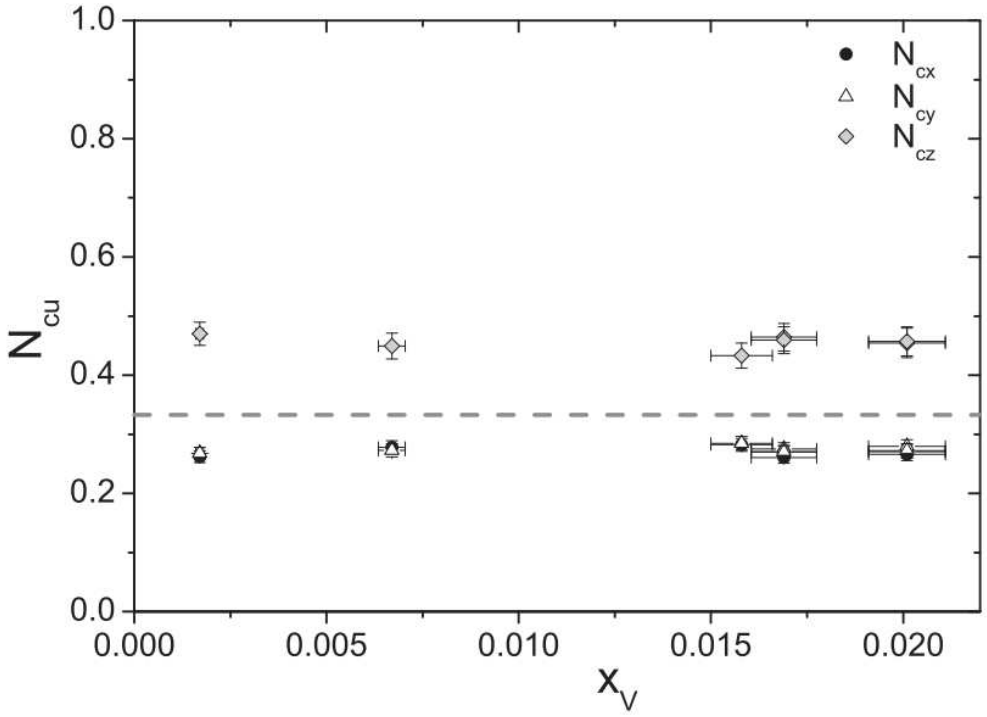

FIG. 20. Cluster demagnetizing factors N_{cu}, as a function of NPs volume fraction x_V. Dashed line stands for the expected value for random cluster orientations, $N_{cu} = 1/3$.

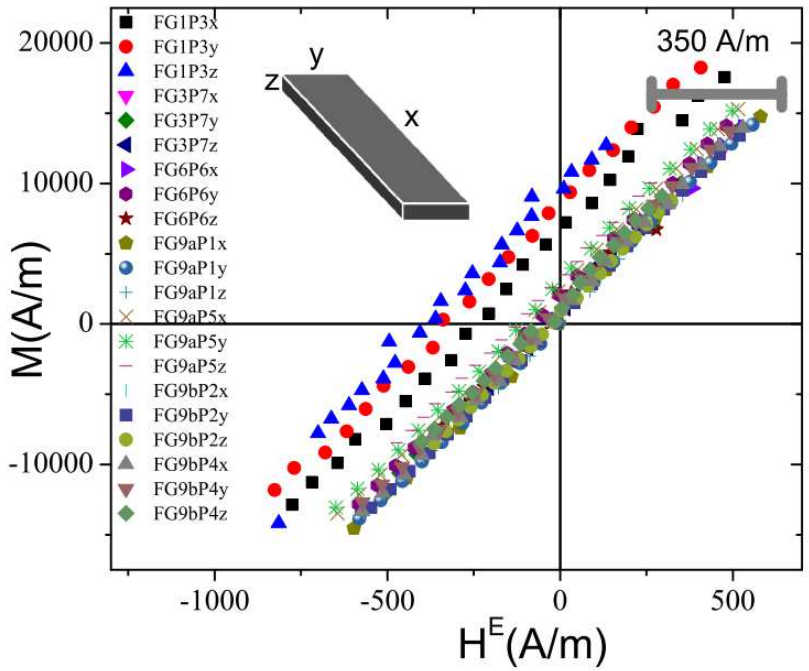

FIG. 21. Linear part of room temperature M vs. H^E cycles for all of the specimens, after correcting by demagnetizing effects.